J. Membrane Biol. 110, 67–86 (1989)

The Journal of
Membrane Biology

Conformational Transitions and Charge Translocation by the Na,K Pump: Comparison of Optical and Electrical Transients Elicited by ATP-Concentration Jumps

W. Stürmer, H.-J. Apell, I. Wuddel, and P. Läuger
Department of Biology, University of Konstanz, D-7750 Konstanz, Federal Republic of Germany

Summary. The electrogenic properties of the Na,K-ATPase were studied by correlating transient electrical events in the pump molecule with conformational transitions elicited by an ATP-concentration jump. Flat membrane fragments containing a high density (~8000 μm^{-2}) of oriented Na,K-ATPase molecules were bound to a planar lipid bilayer acting as a capacitive electrode. ATP was released in the medium from a photolabile inactive ATP derivative ("caged" ATP) by a 40-μsec light flash. Electrical signals resulting from transient charge movements in the protein under single-turnover conditions were recorded in the external measuring circuit. In parallel experiments carried out under virtually identical conditions, the fluorescence of membrane fragments containing Na,K-ATPase with covalently-bound 5-iodoacetamido-fluorescein (5-IAF) was monitored after the ATP-concentration jump. When the medium contained Na^+, but no K^+, the fluorescence of the 5-IAF-labeled protein decreases monotonously after release of ATP. In the experiments with membrane fragments bound to a planar bilayer, a transient pump current was observed which exhibited virtually the same time behavior as the fluorescence decay. This indicates that optical and electrical transients are governed by the same rate-limiting reaction step. Experiments with chymotrypsin-modified Na,K-ATPase suggest that both the fluorescence change as well as the charge movement are associated with the deocclusion of Na^+ and release to the extracellular side. In experiments with Na^+-free K^+ media, a large inverse fluorescence change is observed after the ATP-concentration jump, but no charge translocation can be detected. This indicates that deocclusion of K^+ is an electrically silent process.

Key Words Na,K-ATPase · active transport · electrogenic pumps · fluorescence probes · conformational transitions · caged ATP

Introduction

The Na,K pump of the plasma membrane of animal cell utilizes free energy of ATP hydrolysis for uphill transport of Na^+ and K^+ (Skou, 1975; Robinson & Flashner, 1979; Cantley, 1981; Schuurmans-Stekhoven & Bonting, 1981; Jørgensen, 1982; Glynn, 1985; Kaplan, 1985; Jørgensen & Andersen, 1988). In its normal mode of operation, the pump performs a cycle of conformational transitions and ion-binding and -release steps. Spectroscopic studies as well as proteolysis experiments indicate that the enzyme can assume two principal conformations designated E_1 and E_2. Form E_1 has the ion-binding sites facing the cytoplasm and is stabilized by Na^+; form E_2 has the ion-binding sites facing the extracellular medium and is stabilized by K^+. From enzymatic and transport studies the reaction cycle represented in Fig. 1 has been proposed (Albers, 1967; Post, Hegyvary & Kume, 1972; Cantley et al., 1984). When the protein is phosphorylated in state E_1 by ATP, Na^+ becomes "occluded," i.e., trapped inside the protein ($Na_3 \cdot E_1 \cdot ATP \rightarrow (Na_3)E_1{-}P$). After transition to conformation E_2, Na^+ is released and K^+ is bound. This leads to dephosphorylation of the protein and occlusion of K^+. The original state is restored by transition to conformation E_1 and release of K^+ to the cytoplasmic side.

The kinetics of transitions between conformations E_1 and E_2 may be investigated by time-resolved fluorescence measurements, using intrinsic or extrinsic fluorescent probes (Karlish & Yates, 1978; Karlish, Yates & Glynn, 1978*a*,*b*; Karlish, 1980; Hegyvary & Jørgensen, 1981; Skou & Esmann, 1981, 1983; Skou, 1982; Taniguchi, Suzuki & Iida, 1983; Rephaeli, Richards & Karlish, 1986*a*,*b*; Glynn et al., 1987; Suzuki, Taniguchi & Iida, 1987). These studies have shown that transitions from E_1 to E_2 may be induced by changing the medium from a sodium-rich to a potassium-rich solution (and vice versa), or by phosphorylation. From the time course of fluorescence changes, estimates for the rate constants of the reaction cycle may be obtained.

An entirely different possibility for studying the kinetics of the pumping process consists in analyzing electrical signals resulting from charge translocations in the pump molecule. Flat membrane fragments containing a high density (several thousand

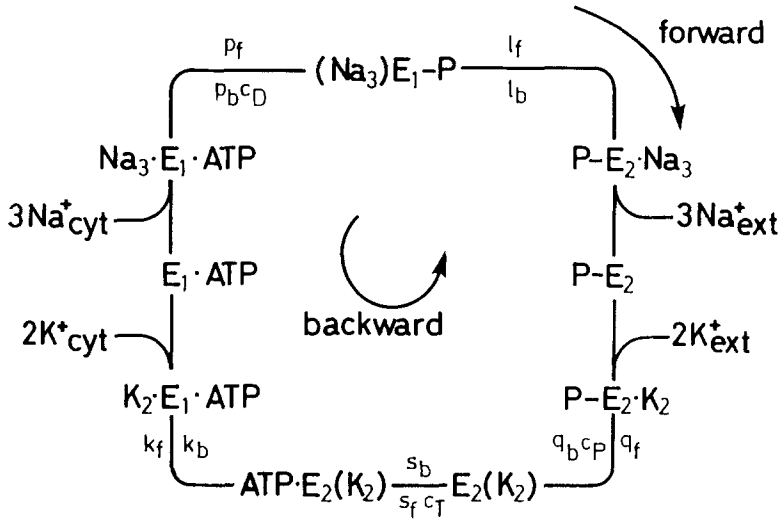

Fig. 1. Post-Albers scheme for the pumping cycle of Na,K-ATPase (adapted from Cantley et al., 1984). E_1 and E_2 are conformations of the enzyme with ion binding sites exposed to the cytoplasm and the extracellular medium, respectively. In the "occluded" states $(Na_3)E_1-P$ and $E_2(K_2)$ the bound ions are unable to exchange with the aqueous phase. Dashes indicate covalent bonds and dots indicate noncovalent bonds. p_f, l_f, q_f, $s_f c_T$, k_f and $p_b c_D$, k_b, s_b, $q_b c_P$, l_b are rate constants for transitions in forward and backward direction, respectively. c_T, c_D and c_P are cytoplasmic concentrations of ATP, ADP and P_i (inorganic phosphate)

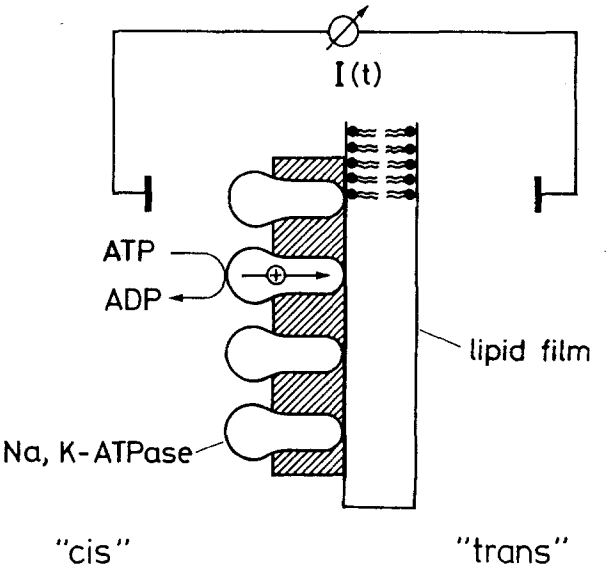

Fig. 2. Planar lipid bilayer with adsorbed Na,K-ATPase membrane fragments. When a suspension of flat membrane fragments 0.1–1 μm in diameter containing a high density (10^3–10^4 μm^{-2}) of oriented Na,K-ATPase molecules is added to the aqueous medium, membrane fragments become bound to the lipid bilayer, some with the cytoplasmic side facing the solution. Flash-induced release of ATP from a photolabile ATP derivative ("caged" ATP) elicits a transient current $I(t)$ in the external measuring circuit

per μm^2) of oriented Na,K-ATPase molecules may be bound to a planar lipid bilayer acting as a capacitive electrode (Fig. 2). When ATP is released within a few msec to the medium by flash excitation of a photolabile inactive ATP-derivative ("caged" ATP) current signals can be recorded in the external measuring circuit in the time range of 10–100 msec (Fendler et al., 1985; Apell, Borlinghaus & Läuger, 1987; Borlinghaus, Apell & Läuger, 1987; Fendler, Grell & Bamberg, 1987; Nagel et al., 1987; Borlinghaus & Apell, 1988). These transient currents reflect charge movements in the protein induced by phosphorylation. Blocking the deocclusion step $(Na_3)E_1-P \rightarrow P-E_2 \cdot Na_3$ by chymotrypsin modification of the protein has given evidence that the main electrogenic step in the sodium limb of the cycle is deocclusion of Na^+ to the extracellular side (Borlinghaus et al., 1987).

An important problem in the understanding of the kinetic behavior of the Na,K-pump is the question, how the charge movements which give rise to the transient currents are correlated with the spectroscopically-detected conformational changes. In the following, we describe experiments in which transient fluorescence changes of 5-iodoacetamidofluorescein-labeled Na,K-ATPase (Kapakos & Steinberg, 1982, 1986*a*,*b*; Glynn et al., 1987; Fortes & Aguilar, 1988; Steinberg & Karlish, 1989; Tyson et al., 1989) have been recorded after an ATP-concentration jump. In parallel experiments with the same ATPase preparation, electrical signals have been measured in the lipid bilayer system after flash release of ATP from "caged" ATP. It will be shown that valuable kinetic information can be obtained by comparison of the optical and the electrical signals.

Materials and Methods

Materials

L-1,2-diphytanoyl-3-phosphatidylcholine was obtained from Avanti Polar Lipids, Birmingham, AL; sodium dodecylsulfate (SDS) from Pierce Chemical (Rockford, IL) and sodium cholate from Merck (Darmstadt). Phosphoenolpyruvate, pyruvate ki-

nase, lactate dehydrogenase, luciferin, luciferase, NADH and ATP (disodium salt, Sonderqualität) were from Boehringer (Mannheim). α-chymotrypsin (type II), apyrase VI and ouabain were purchased from Sigma and 5-iodoacetamidofluorescein (5-IAF) from Molecular Probes (Eugene, OR). In the experiments in nominal absence of K^+, NaCl was used in Suprapur quality (Merck). All other reagents were analytical grade. Sephadex G25 and G100 were obtained from Serva (Heidelberg).

P^3 - 1 - (2 - nitro)phenylethyladenosine - 5' - triphosphate ("caged" ATP) was synthetized by K. Janko using a modified version of the method of Kaplan, Forbush and Hoffman (1978). The purity of the product was checked by HPLC. The compound was stored as tetramethylammonium salt in the dark at −40°C.

Enzyme Preparation and Fluorescence Labeling

Na,K-ATPase was prepared from the outer medulla of rabbit kidneys using procedure C of Jørgensen (1974). This method yields purified enzyme in the form of membrane fragments containing about 0.6 mg phospholipid and 0.2 mg cholesterol per mg protein (Jørgensen, 1974, 1982). The specific ATPase activity was determined by the pyruvate kinase/lactate dehydrogenase assay (Schwartz et al., 1971) and the protein concentration by the Lowry method (Lowry et al., 1951), using bovine serum albumin as a standard. For most preparations the specific activity was in the range between 1500 and 2200 μmol P_i per hr and mg protein at 37°C, corresponding to a turnover rate of 120–170 sec^{-1} (based on a molar mass of 280,000 g/mol). The suspension of Na,K-ATPase-rich membrane fragments (about 3 mg protein per ml) in buffer (25 mM imidazole, pH 7.5, 1 mM EDTA, 10 mg/ml saccharose) was frozen in samples of 100 μl; in this form the preparation could be stored for several months at −70°C without significant loss of activity.

Fluorescence labeling of the enzyme was performed by incubating 200–300 μg of the enzyme for 48 hr at 4°C with a solution containing 100 μM 5-IAF, 10 mM K_2SO_4 and 50 mM imidazole sulfate, pH 7.5 (Kapakos & Steinberg, 1982). The labeled enzyme was separated from unbound dye by passing the reaction mixture through a 3-cm long Sephadex G-25 column.

Fluorescence Measurements

For high-resolution recording of time-dependent fluorescence signals the set-up represented in Fig. 3 was used. The fluorescence of membrane-bound 5-IAF was excited by light from a 250-W tungsten-halogen lamp. The light beam passed through a water-filled infrared-absorbing filter (*not shown*) and an interference filter (peak wavelength 481 nm, half-width 14 nm; Anders, Nabburg, FRG). The exciting light was focussed into the cylindrical quartz cuvette (internal diameter 7.8 mm). The solution layer in the cuvette had a height of 5–6 mm. The bottom plate of the cuvette was coated at the outer surface with a reflecting layer; it was in contact with a thermostated metal console of the same diameter as the cuvette. Fluorescence light emitted from the cuvette was collected by an ellipsoidal mirror (Melles Griot, Zevenaar, Netherlands) and focussed onto the cathode of a side-on photomultiplier (Hamamatsu, Mod. R928). Cuvette and photomultiplier were mounted in such a way that the light-emitting part of the cuvette was in one focal point of the mirror and the photocathode in the other. In this way efficient light collection from a large solid angle was achieved. A second interference

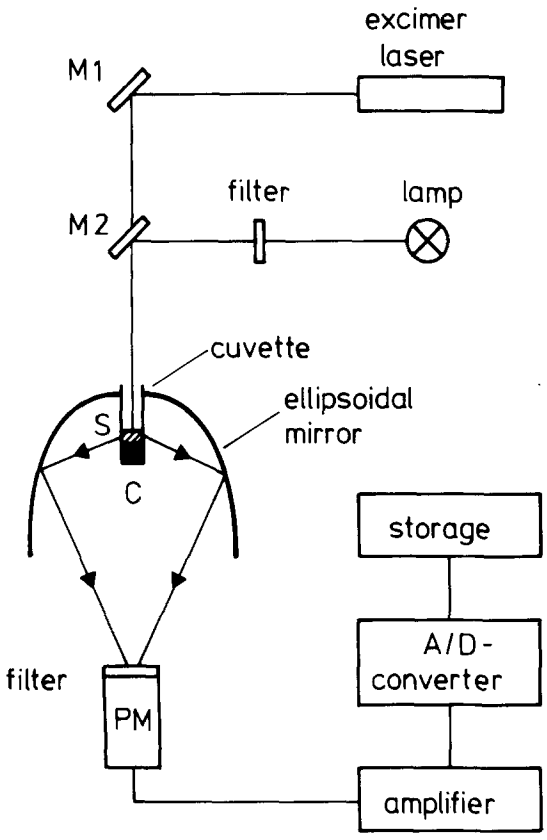

Fig. 3. Set-up for time-resolved fluorescence measurements. The cylindrical glass cuvette containing the sample (*S*) is mounted on a thermostated metal console (*C*). Fluorescence of the sample is excited by light from a tungsten-halogen lamp. The light emitted by the sample is collected by an ellipsoidal mirror and focussed onto the cathode of the photomultiplier (*PM*). The light-emitting part of the cuvette is located in one focal point of the mirror and the photocathode in the other. The photomultiplier signal is amplified, digitized in an analog-to-digital converter and stored in the memory of the Compaq-386 computer. ATP is released from "caged" ATP by a 10-nsec pulse from an excimer laser. The laser beam enters the cuvette through a hole in mirror *M2*

filter (peak wavelength 522.5 nm, half-width 12.6 nm) was mounted in front of the photomultiplier.

The voltage for the photomultiplier was delivered by a highly stabilized power supply (John Fluke, Seattle, Mod. 405B). The current signal of the photomultiplier was converted to voltage and amplified in three stages. The input stages of the amplifiers were protected by diodes against overload. This was necessary since the 308-nm flash excited strong fluorescence and phosphorescence in some of the optical elements (lenses and cuvette). The total recovery time of the recording system after the flash was given by the decay time constant of the phosphorescence (~1 msec). For the compensation of the stationary fluorescence signal prior to the flash a differential amplifier was used. The output signal of the differential amplifier was amplified ten times and passed through an active low-pass filter. In most experiments the bandwidth was 1 kHz. The filtered signal was digitized with a 12-bit analog-to-digital converter (RC-Electronics,

Santa Barbara, CA, Mod. ISC-16) and stored on the hard disk of the Compaq-386 computer.

The cuvette was filled with 200–300 μl of a suspension of labeled membrane fragments (usually about 5 μg protein per ml) in a medium containing 30 mM imidazole buffer, pH 7.2, and 1 mM EDTA.

Photochemical Release of ATP in the Fluorescence Cuvette

Light flashes (wavelength: 308 nm; total energy: 150 mJ; duration: 10 nsec) were generated with a EMG 100 excimer laser (Lambda Physics, Göttingen). At pH 7.0, ATP is liberated from "caged" ATP (cg-ATP) with a time constant of 4.6 msec (McCray et al., 1980). The concentration of released ATP was determined by the luciferin/luciferase test which was calibrated using solutions of known ATP concentration (De Luca & McElroy, 1978; Ernst, Böhme & Böger, 1983). If not otherwise stated, the concentration of cg-ATP was 100 μM. About 15–25 μM ATP were released in a single flash, corresponding to a photochemical yield of 15–25%.

Care had to be taken to avoid spatial inhomogeneities in the concentration of released ATP in the fluorescence cuvette, since concentration gradients of ATP can lead to distortions in the time course of the optical signal. Even if the light intensity is sufficiently constant over the cross section of the laser beam, intensity gradients in the direction of propagation may result from light absorption in the solution. At 308 nm, cg-ATP has an extinction coefficient of about 2000 M^{-1} cm^{-1} (*unpublished data*). This means that the path length for an *e*-fold change of light intensity is 22 mm at a concentration of 100 μM. When the height of the solution layer in the cuvette is 6 mm, a maximum intensity variation by a factor of 1.3 may be expected. Part of this intensity variation was eliminated by back reflection from the mirror at the bottom of the cuvette. Effects of concentration gradients of ATP may be estimated to be negligible in the experiments in which ATP binds to the high affinity site. Since the dissociation constant of ATP at the high affinity site is of the order of 0.1–1 μM, the binding sites are almost completely saturated at a concentration of released ATP of 15–25 μM, independent of small variations in the ATP concentration within the cuvette. In the experiments with sodium-free K^+ solutions, in which ATP acts at a low-affinity site, errors introduced by distortion of the fluorescence signal have to be taken into account.

Recording of Electrical Signals

Optically black films were formed from a solution of 10 mg/ml diphytanoylphosphatidylcholine in *n*-decane (Läuger et al., 1967; Borlinghaus et al., 1987). The membrane cell which was made of Teflon consisted of two compartments separated by a thin Teflon septum with a circular hole of 1.3 mm diameter. One compartment could be completely closed after filling with the aqueous solution; this increased the mechanical stability of the membrane and allowed efficient stirring in the open compartment (*cis* side) to which Na,K-ATPase membrane fragments were added (Fig. 2). The solution volumes of the closed and the open compartments were 5 and 0.3 ml, respectively. The Teflon cell was enclosed in a thermostated metal block with openings for the entry of the UV-light beam and for visual observation of the membrane. The area of the black film was measured with an eye-piece micrometer.

The solutions on either side of the lipid membrane were connected to the external measuring circuit via agar bridges and silver/silver-chloride electrodes. In order to minimize stray-light artifacts from the electrodes, a suspension of carbon-black was added to the agar. For current measurements under short-circuit conditions, the signal was amplified with a Keithley Mod. 427 current amplifier, with the risetime usually set at 3 msec. For measuring voltage signals, a Mod. 3528 Burr-Brown amplifier with an input impedance of 10^{12} Ω was used. The signals were recorded with a digital oscilloscope (Nicolet Mod. 4094 A) and stored on diskettes. The membrane cell and the electrodes were enclosed in a Faraday shield.

If not otherwise indicated, the aqueous solutions contained 30 mM imidazole, pH 7.2, 10 mM $MgCl_2$, and various concentrations of NaCl and KCl. "Caged" ATP (usually 0.24 mM) and membrane fragments (about 40 μg protein/ml) were added together to the open compartment (*cis* side) under stirring. The stirring was continued for about 1 min. Electrical signals were recorded 20–30 min after addition of membrane fragments to the cell.

Light flashes of 40 μsec duration and a total energy of 5 J were generated with a Xenon flash-tube (Mod. 5M-3) from EG&G Electro-Optics (Salem, MA). The emitted light passed through a bandpass filter with >50% transparency between 260 and 380 nm (Schott, Mainz, Mod. UG11). The light beam entered the cell from the *trans* side (Fig. 2) and was focussed onto the membrane.

Results

Fluorescence Signals in the Presence of Na^+

Intrinsic Dye Response

When a suspension of 5-IAF-labeled membrane fragments in K^+-free Na^+ buffer was irradiated by a 308-nm laser flash in the presence of a blocking concentration (500 μM) of ouabain, a fast decrease of fluorescence intensity by 3–5% was observed, followed by a slow recovery to about 99% of the original level within 50 msec (Fig. 4*A*). Repetitive flashes led to a gradual bleaching of the fluorescent dye. A nearly identical flash-induced fluorescence signal was observed without ouabain, when either caged ATP or Mg^{2+} or Na^+ were omitted from the solution. The origin of this intrinsic dye response is not clear so far; it may result from transient formation of an oxidized intermediate of the dye (Lindqvist, 1960). Degassing the solution only slightly reduced the amplitude of the signal. A similar bleaching artifact, but with faster recovery (within about 10 msec) was observed with a solution of 15 nM 5-IAF in buffer without membrane fragments (*not shown*).

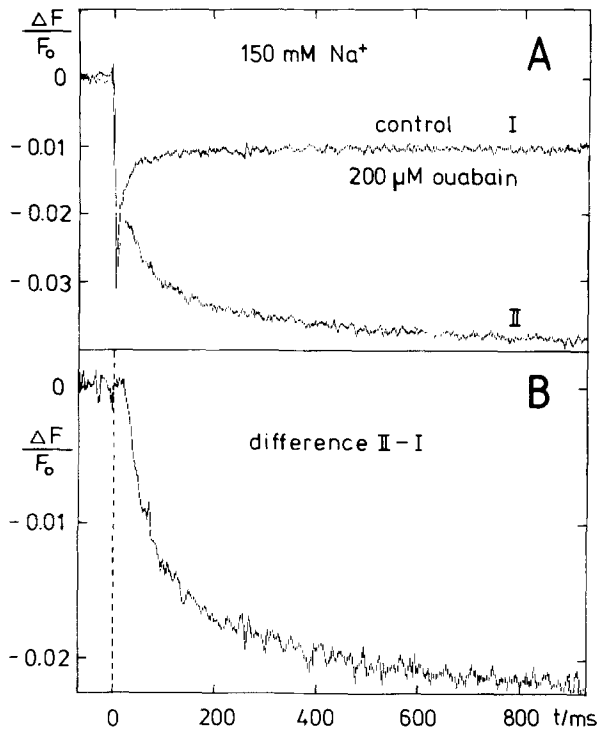

Fig. 4. Relative fluorescence change $\Delta F/F_0$ under K^+-free conditions as a function of time t after a 308-nm light-flash of 10 nsec duration given at time $t = 0$. F_0 is the fluorescence intensity prior to the flash. Excitation wavelength: 481 nm; emission wavelength: 523 nm. The temperature was 20°C. (*A*) Suspension of 5-IAF-labeled membrane fragments (about 5 μg protein/ml) in 30 mM imidazole, pH 7.2, 1 mM EDTA, 150 mM NaCl, 10 mM $MgCl_2$ and 100 μM caged ATP. In the control experiments (curve *I*), 500 μM ouabain was added. The concentration of released ATP was estimated to be about 20 μM. (*B*) difference *II-I*

Fluorescence Signals Associated with Pump Activity

For each set of experiments, a control experiment was carried out in which the time course of the intrinsic dye response described above was recorded under conditions under which pump activity was inhibited (Fig. 4*A*). Pump inhibition was achieved by adding a saturating concentration (500 μM) of ouabain, or (in the experiments with K^+ media) by omitting Mg^{2+}. The control signal was stored and was substracted from the fluorescence signals observed in the normal experiment (Fig. 4*B*).

The difference signal in Fig. 4*B* exhibits a short lag phase followed by a nearly exponential decay with a time constant of $\tau \approx 50$ msec. The observed drop of fluorescence after addition of ATP in the presence of Na^+ and Mg^{2+} qualitatively agrees with previous findings of Kapakos and Steinberg (1986*b*). The maximal fluorescence change, $\Delta F(t \to \infty)/F_0$, in our experiments with rabbit kidney enzyme is smaller than observed by Kapakos and Steinberg with dog enzyme (about 2–3% for rabbit enzyme at 5 mM Na^+ compared to ≈7% for dog enzyme under similar conditions).

The lag phase of the fluorescence signal after the ATP concentration jump is likely to be determined by the finite rates of photochemical release and binding of ATP to the protein (Apell et al., 1987; Borlinghaus & Apell, 1988). The rate constant of release of ATP from caged ATP is about 140 sec^{-1} at pH 7.2 and 22°C (McCray et al., 1980). Caged ATP is known to bind to the ATP site of Na,K-ATPase with an equilibrium dissociation constant estimated in the range of 30–500 μM (Forbush, 1984; Nagel et al., 1987; Borlinghaus & Apell, 1988), whereas ATP binds to the E_1 form of the enzyme with much higher affinity (dissociation constant 0.1–1 μM). Accordingly, ATP released in the aqueous solution has to compete with caged ATP bound to the ATP site of the enzyme. Furthermore, bound caged-ATP may be transformed into ATP in situ. It has been shown previously (Borlinghaus & Apell, 1988) by numerical simulation that the finite rate of the reactions preceding phosphorylation may be described by an effective time constant of ATP release and binding of about 20–50 msec under the experimental conditions of Fig. 4. This time constant approximately agrees with the observed lag time in Fig. 4*B*. However, because of the bleaching artifact, the exact shape of the intrinsic fluorescence signal is difficult to determine in the time range of 0–30 msec. Reliable information may be obtained from the decay of the fluorescence signal at times $t > 30$ msec.

Previous studies indicate that phosphorylation by ATP in the absence of K^+ leads to the reaction sequence $Na_3 \cdot E_1 \cdot ATP \to (Na_3)E_1{-}P \to P{-}E_2 \cdot Na_3 \to P{-}E_2$ (Glynn, 1985). Under K^+-free conditions, $P{-}E_2$ is a long-lived state, which only slowly (with a rate constant $r_f \approx 1$–5 sec^{-1}) returns to state E_1. It is therefore likely to assume that the fluorescence decay in Fig. 4*B* reflects the $E_1 \to E_2$ conformational transition of the protein (Kapakos & Steinberg, 1986*a*,*b*). This conclusion is consistent with the results of other fluorescence experiments using intrinsic and extrinsic probes (Karlish & Yates, 1978; Jørgensen & Karlish, 1980; Taniguchi et al., 1983; Glynn et al., 1987).

From direct measurements of the rates of phosphorylation and dephosphorylation (Mårdh & Zetterquist, 1974; Mårdh, 1975) it is known that the transition $Na_3 \cdot E_1 \cdot ATP \to (Na_3)E_1{-}P$ is much faster than the subsequent deocclusion step

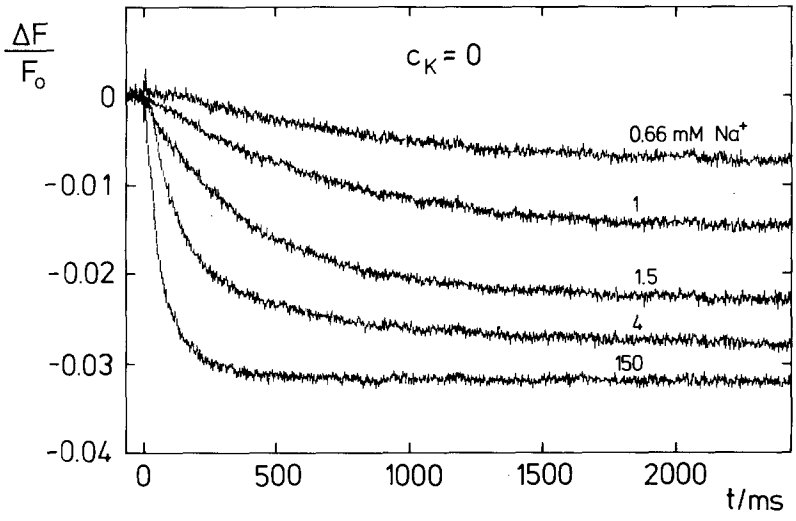

Fig. 5. Relative fluorescence change $\Delta F/F_0$ as a function of time t for different Na^+ concentrations (0.66, 1, 1.5, 4 and 150 mM) and 5 mM Mg^{2+}. At time $t = 0$, about 20 μM ATP were released in the solution. The other experimental conditions were the same as in Fig. 4

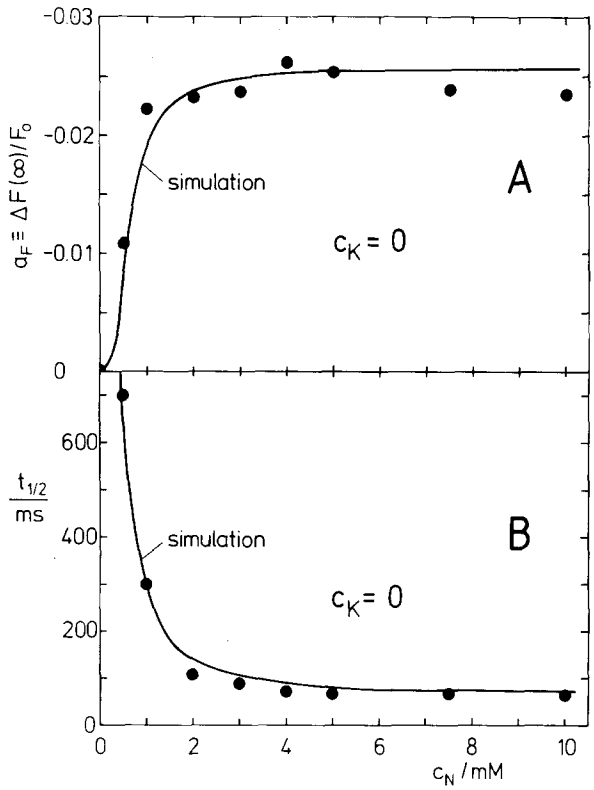

Fig. 6. Amplitude $a_F \equiv \Delta F(\infty)/F_0$ and half-time $t_{1/2}$ of the ATP-induced fluorescence decrease (Fig. 5) under K^+-free conditions as a function of Na^+ concentration c_N. $t_{1/2}$ is the time at which $\Delta F/F_0$ reaches the half-maximal value $a_F/2$. Experimental data are represented by circles. The lines have been obtained by numerical simulation of the reaction cycle of Fig. 15, using the parameter values of the Table (*see* text). a_F was corrected for the intrinsic fluorescence change of the dye, as described in the legend of Fig. 4. The experimental conditions were the same as in the experiments of Fig. 5

$[(Na_3)E_1 \cdot ATP \rightarrow P\text{–}E_2 \cdot Na_3]$. If the fluorescence of states $Na_3 \cdot E_1 \cdot ATP$ and $(Na_3)E_1\text{–}P$ is different, then a fast fluorescence change should precede the slow decay of the signal. Since such a fast component of the signal is not observed (Fig. 4*B*), it is likely to assume that states $Na_3 \cdot E_1 \cdot ATP$ and $(Na_3)E_1\text{–}P$ have similar fluorescence properties. The sensitivity by which fast fluorescence changes can be detected is limited, however, by the intrinsic dye response (Fig. 4*A*) and by the finite rate of the reactions preceding phosphorylation. More direct support for the assumption that the transition $Na_3 \cdot E_1 \cdot ATP \rightarrow (Na_3)E_1\text{–}P$ does not contribute to the fluorescence signal comes from experiments with chymotrypsin-modified enzyme (*see below*).

The time course of the ATP-induced fluorescence change $\Delta F/F_o$ is shown in Fig. 5 for the different Na^+ concentrations (0.66, 1, 1.5, 4 and 150 mM). $\Delta F(t)/F_o$ can be approximately fitted by a single exponential function with a time constant depending on sodium concentration. Occasionally, fluorescence signals were observed in which the initial decay of $\Delta F/F_o$ was followed by a slower decrease extending over the time range of 1–2 sec. These biphasic signals, which were obtained with a few Na,K-ATPase preparations under otherwise identical conditions, were not analyzed further.

The amplitude $a_F \equiv \Delta F(\infty)/F_o$ and the half-time $t_{1/2}$ of the fluorescence signal are plotted as functions of Na^+ concentration c_N in Fig. 6. $t_{1/2}$ is the time at which $\Delta F/F_o$ reaches the half-maximal value $a_F/2$. As seen from Fig. 6*B*, $t_{1/2}$ steeply decreases with increasing Na^+ concentration. This has to be expected, since the rate of ATP-induced conformational change $E_1 \rightarrow E_2$ is proportional to the concentration of $Na_3 \cdot E_1$ which becomes small at low so-

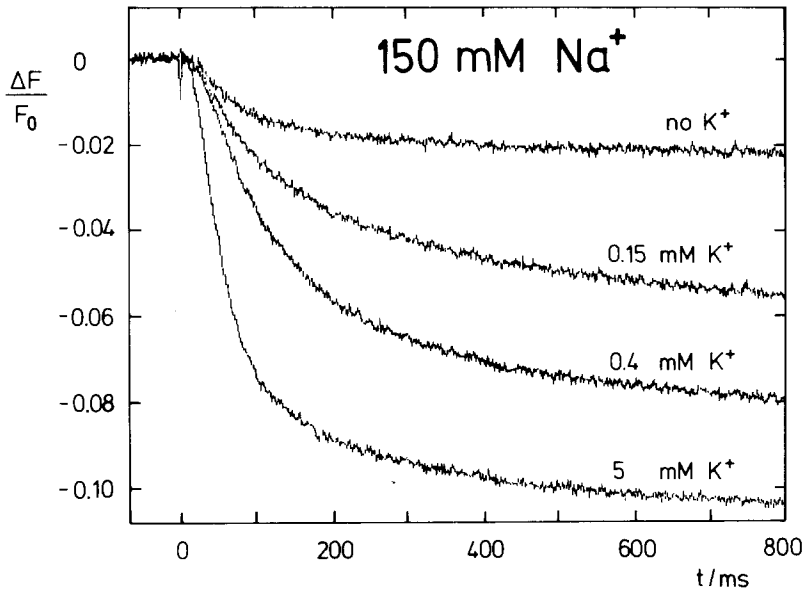

Fig. 7. Relative fluorescence change $\Delta F/F_0$ as a function of time t in the presence of Na^+ and K^+. At time = 0 about 20 μM ATP was photochemically released. The medium contained 5-IAF-labeled membrane fragments (5 μg protein/ml), 30 mM imidazole, 1 mM EDTA, pH 7.2, 100 μM caged ATP, 5 mM Mg^{2+}, 150 mM NaCl, and various concentrations of KCl; T = 20°C. $\Delta F/F_0$ was corrected for the intrinsic fluorescence change of the dye

dium concentration. This explanation agrees with the results of numerical simulations of the reaction cycle (continuous line in Fig. 6*B*) to be discussed in detail later.

In the same Na^+-concentration range (0–3 mM) in which $t_{1/2}$ decreases, the amplitude a_F of the signal increases towards a limiting value. This behavior, which has already been observed by Kapakos and Steinberg (1986*b*) in stationary experiments, results from the fact that at low Na^+ concentration, release of ATP leads only to minor shift in the E_1/E_2 concentration ratio due to spontaneous back reaction $E_2 \rightarrow E_1$ (*see below*).

Chymotrypsin-Modified Enzyme

Treatment of Na,K-ATPase with α-chymotrypsin in the presence of Na^+ at low ionic strength leads to cleavage of a single peptide bond in the α-subunit; the split is located in the cytoplasmic portion of the protein between Leu-266 and Ala-267 (Jørgensen & Collins, 1986). In the chymotrypsin-treated enzyme, phosphorylation by ATP, occlusion of Na^+ and ADP/ATP exchange are preserved, while Na^+,K^+ pumping and Na^+,Na^+ exchange are abolished (Glynn, Hara & Richards, 1984; Jørgensen & Petersen, 1985). These findings indicate that modification by chymotrypsin stabilizes the enzyme in the E_1 conformation by preventing the $E_1 \rightarrow E_2$ transition.

5-IAF-labeled membrane fragments (about 300 μg/ml) were incubated for 10–30 min at 30°C in a medium containing 10–20 μg/ml α-chymotrypsin, 10 mM NaCl and 15 mM imidazole, pH 7.5 (Jørgensen & Petersen, 1985). Under these conditions the proteolytic reaction may be expected to be selective, consisting in the cleavage of a single peptide bond, as mentioned above. After incubation, the membrane fragments were separated from the medium on a Sephadex G100 column. When the ATP-concentration jump experiment was done with the chymotrypsin-modified Na,K-ATPase under the conditions of Fig. 4, no fluorescence change was observed, apart from the intrinsic dye response. This finding agrees with recent observations from stopped-flow experiments with 5-IAF-labeled Na,K-ATPase (Steinberg & Karlish, 1989). In accordance with the results presented in the previous section, we may thus conclude that the transition $Na_3 \cdot E_1 \cdot ATP \rightarrow (Na_3)E_1{-}P$ does not contribute to the fluorescence signal.

The most likely explanation of the experiment of Fig. 4*B* therefore consists in the assumption that the observed fluorescence decay results from the deocclusion step $(Na_3)E_1{-}P \rightarrow P{-}E_2 \cdot Na_3$, followed by release of Na^+ from the extracellular binding sites.

Fluorescence Signals in Presence of Na^+ and K^+

When, in the presence of a high concentration of Na^+, millimolar quantities of K^+ are added to the medium, the amplitude of the ATP-induced signal strongly increases, while the time course of the fluorescence decay (at high sodium concentration) does not appreciably change (Fig. 7). The dependence of signal amplitude a_F and of half-time $t_{1/2}$ on potas-

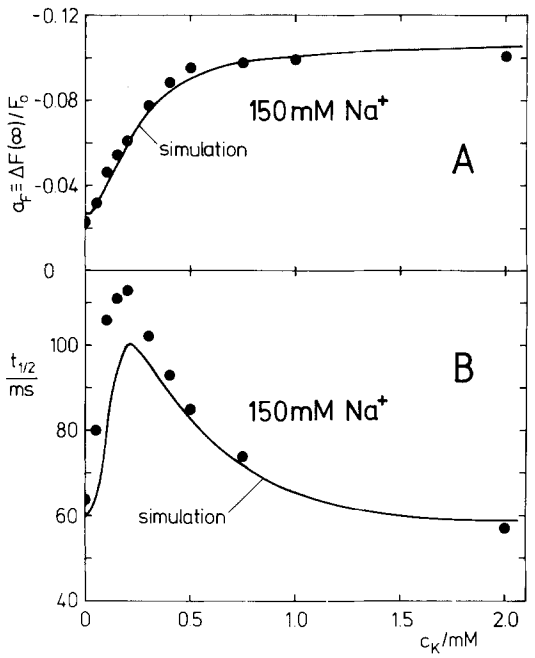

Fig. 8. Amplitude $a_F \equiv \Delta F(\infty)/F_0$ and half-time $t_{1/2}$ of the ATP-induced fluorescence decrease in the presence of 150 mM Na^+ as a function of K^+ concentration c_N. $t_{1/2}$ is the time at which $\Delta F/F_0$ reaches the half-maximal value $a_F/2$. Experimental data are represented by circles. The lines have been obtained by numerical simulation of the reaction cycle of Fig. 15, using the parameter values of the Table (*see* text). a_F was corrected for the intrinsic fluorescence change of the dye, which was recorded in the absence of Na^+ and K^+. Apart from c_K, the conditions were the same as in the experiments of Fig. 7

sium concentration c_K is shown in Fig. 8 together with the results of numerical simulations of the reaction cycle (full lines). The amplitude a_F exhibits a saturation behavior while the half-time $t_{1/2}$ increases from about 60 msec towards a peak value of ≈110 msec and thereafter decreases again.

The effect of K^+ on the ATP-induced fluorescence change may be explained in the following way. In the experiments represented in Figs. 7 and 8, the concentration of flash-released ATP (≈20 μM) was much smaller than the dissociation constant of ATP at the low-affinity binding site, which is about 0.5 mM (Robinson & Flashner, 1979). Under this condition, phosphorylation of the enzyme mainly populates state $E_2(K_2)$ via the reaction sequence $P{-}E_2 \cdot Na_3 \rightarrow P{-}E_2 \cdot K_2 \rightarrow E_2(K_2)$, since at low ATP concentration the transition $E_2(K_2) \rightarrow K_2 \cdot E_1$ is extremely slow (Glynn, 1985). Accordingly, if state $E_2(K_2)$ has a lower fluorescence than state $P{-}E_2$ (Kapakos & Steinberg, 1986*b*), the total fluorescence decrease becomes larger when the protein is phosphorylated in the presence of K^+. The lack of a large effect of K^+ on the time behavior of the signal may be explained, assuming that the rate-limiting step in the reaction sequence $E_1 \rightarrow \cdots \rightarrow E_2(K_2)$ is the deocclusion of Na^+, both in the absence and in the presence of millimolar concentrations of K^+. This assumption is substantiated by numerical simulations of the reaction cycle, as will be discussed later.

Fluorescence Signals in the Presence of K^+

When the medium contains K^+, but not Na^+, an ATP-concentration jump leads to a fluorescence increase, i.e., to a signal of opposite polarity compared to the signals observed with Na^+ media (Fig. 9). For $t > 20$ msec, the time course of the fluorescence change can be approximately described by a simple exponential relation of the form $\Delta F/F_o = a[1 - \exp(-t/\tau)]$. In the absence of Na^+, ATP acts on the low-affinity nucleotide-binding site, so that at the given concentration of photochemically released ATP (≈20 μM), the photoresponse remains far from saturation. This means that $\Delta F(t)/F_o$ may be affected by inhomogeneities in ATP concentration resulting from spatial variations of laser-light intensity. For this reason the values of amplitude a_F and time constant τ of the signal represent averages over a range of ATP concentrations.

As seen from Fig. 10, the signal amplitude a_F increases with increasing K^+ concentration c_K up to a maximum and thereafter decreases again. The positive value of a_F is consistent with the assumption discussed in the previous section that $E_2(K_2)$ has a lower fluorescence than E_1. In the presence of millimolar concentrations of K^+ and in the absence of Na^+ and ATP, a substantial fraction of the enzyme is initially present in state $E_2(K_2)$, since the equilibrium between $K_2 \cdot E_1$ and $E_2(K_2)$ is strongly poised (about 1000-fold) towards $E_2(K_2)$ (Karlish, 1980; Karlish & Stein, 1982). Binding of ATP to $E_2(K_2)$ shifts the equilibrium back to state $E_1 \cdot$ ATP, which gives rise to an increase of fluorescence. In the presence of high concentrations of K^+, the enzyme remains mainly in states $K_2 \cdot E_1 \cdot$ ATP and ATP $\cdot E_2(K_2)/E_2(K_2)$ after ATP release, so that the fluorescence change is smaller. These predictions are consistent with the results of numerical simulations of the reaction cycle (continuous line in Fig. 10*A*).

The half-time $t_{1/2}$ of the fluorescence signal $\Delta F(t)/F_o$ decreases from 240 to 60 msec when the K^+ concentration c_K increases from 0.25 to 10 mM (Fig. 10*B*). $(\ln 2)/t_{1/2}$ may be assumed to correspond to the rate constant of the $E_2 \rightarrow E_1$ transition, which, at $c_K = 0.25$ mM, is about 2.9 sec^{-1} under our experimental conditions (concentration of re-

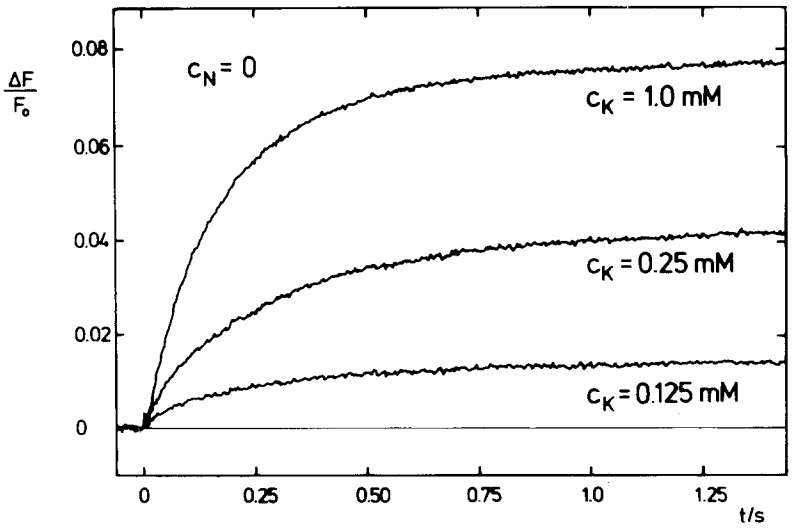

Fig. 9. Fluorescence signal $\Delta F/F_0$ in a sodium-free potassium medium. At time $t = 0$ about 20 μM ATP were released in a solution containing 0.125, 0.25, or 1 mM K^+; T = 20°C. $\Delta F/F_0$ was corrected for the intrinsic fluorescence change of the dye recorded in the absence of Na^+ and K^+. The other experimental conditions were the same as in Fig. 7

leased ATP about 20 μM). This value may be compared with the rate constant reported by Glynn et al. (1987) at 5 μM ATP and 0.1 mM Rb^+ (0.57 sec^{-1} at T = 20°C). At saturating ATP concentrations ($c_T \gg 0.3$ mM) Forbush (1987*a*) observed at 20°C a rate of K^+ release of 45 sec^{-1}, representing a lower limit for the rate of the $E_2 \rightarrow E_1$ transition at high ATP concentration.

The half-time $t_{1/2}$, as well as the amplitude a_F of the fluorescence signal were found to depend on the Mg^{2+} concentration. $t_{1/2}$ increases about 1.7-fold and a_F about 1.4-fold when the Mg^{2+} concentration was increased from 5 to 10 mM.

Transient Electric Currents

Electric Signals in the Presence of Na^+

Membrane fragments labeled with 5-IAF were added together with 240 μM caged ATP to one side of a planar lipid bilayer, as described under Materials and Methods. After a waiting time of 20–30 min, which is probably required for adsorption of membrane fragments, the photoresponse of the system was fully developed. A light pulse of 40 μsec duration which liberated about 25 μM ATP on the *cis* side of the bilayer (Fig. 2) elicited a transient electric current I (Fig. 11). In these experiments the planar lipid bilayer acts as a capacitive element which couples electrical events in the protein layer to the external measuring circuit (Borlinghaus et al., 1987). In the experiment represented in Fig. 11 the aqueous solutions contained Na^+, but no K^+. The sign of the early phase of the current corresponds to

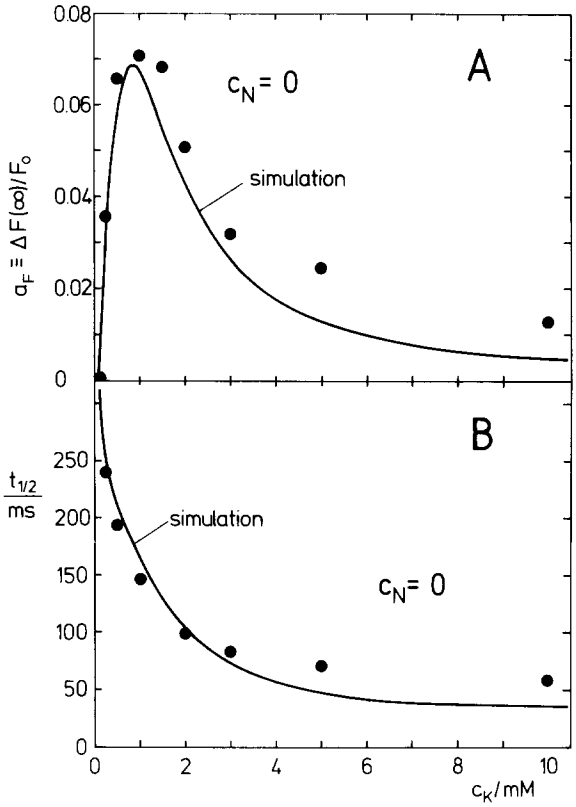

Fig. 10. Amplitude $a_F \equiv \Delta F(\infty)/F_0$ and half-time $t_{1/2}$ of the ATP-induced fluorescence under sodium-free conditions, as a function of potassium concentration c_K. $t_{1/2}$ is the time at which $\Delta F/F_0$ reaches the half-maximal value $a_F/2$. The experimental conditions were the same as in the legend of Fig. 9. Experimental data are represented by circles. The lines have been obtained by numerical simulation of the reaction cycle of Fig. 15, using the parameter values of the Table (*see* text)

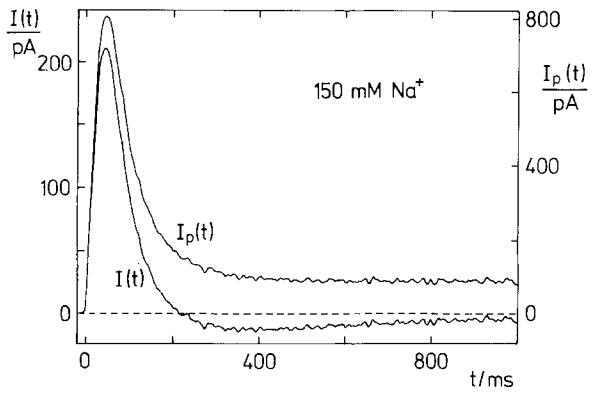

Fig. 11. Current signal $I(t)$ in the absence of K^+ from a lipid bilayer with bound Na,K-ATPase membrane fragments (Fig. 2). At time $t = 0$, about 20 μM ATP was released from caged ATP by a 40-μsec light flash. $I(t)$ was computed from the recorded voltage signal $V(t)$ according to $I(t) = -AC_f dV/dt$. The area A of the black film (specific capacitance $C_f \approx 0.37$ μF/cm^2) was determined by an eye-piece micrometer ($A \approx 0.60$ mm^2). The aqueous solutions contained 150 mM NaCl, 30 mM imidazole, pH 7.2, and 10 mM $MgCl_2$. The temperature was 20°C. Membrane fragments (40 μg/ml) and 240 μM "caged" ATP were added to the *cis* side (Fig. 2) 20 min prior to the experiment. The voltage signal was recorded at a bandwidth of 1 kHz. The intrinsic pump current $I_p(t)$ was evaluated from $I(t)$ according to Eq. (2) of Borlinghaus et al. (1987). The time constant τ_v of the voltage decay at long times, which is required for the evaluation of $I_p(t)$, was determined to be 400 msec

a movement of positive charge from the solution toward the lipid bilayer. The transient current is generated by those membrane fragments that are bound to the bilayer with the cytoplasmic side facing the aqueous medium (Borlinghaus et al., 1987).

Charge translocation after activation of the pump can be detected either as a current $I(t)$ under short-circuit conditions (Fig. 2), or as a voltage $V(t)$. It has been demonstrated previously (Borlinghaus et al., 1987) that voltage and current signals are strictly correlated according to the relation $I(t) = -AC_f dV/dt$, where A and C_f are the area and the specific capacitance of the lipid film, respectively. Since a measurement of $V(t)$ yields a better signal-to-noise ratio, in most experiments voltage signals were recorded. $V(t)$ was subsequently converted into a current $I(t)$ by numerical differentiation. The scaling factor AC_f was estimated by determining the area of the black film with an eye-piece micrometer, using a value of $C_f \approx 0.37$ μF/cm^2 for the specific capacitance (Borlinghaus et al., 1987). Since the absolute magnitude of the current is not used in the subsequent analysis of the electrical signals, errors in the determination of the scaling factor may be neglected.

From the current signal in the external measuring circuit, $I(t)$, the intrinsic pump current $I_p(t)$ can be evaluated. $I_p(t)$ is the current that would be observed in a fictitious experiment in which a continuous layer of membrane fragments is directly interposed (without supporting bilayer) between the aqueous solutions. $I_p(t)$ and $I(t)$ are connected by the circuit parameters of the compound membrane system which may be estimated from the shape of $V(t)$ at long times (Borlinghaus et al., 1987). From Fig. 11 it is seen that $I_p(t)$ and $I(t)$ differ only at large values of t. In particular, the negative phase of $I(t)$ which results from backflow of charge across the shunt conductance of the membrane fragments is not present in $I_p(t)$. Instead, $I_p(t)$ approaches a small quasistationary current I_p^∞ at long times which results from pump molecules undergoing the transition $P{-}E_2 \rightarrow E_1$ and reentering the cycle again (Apell et al., 1987). The small amplitude of I_p^∞ is consistent with the observation that the rate of the transition $P{-}E_2 \rightarrow E_1$ is extremely low (1–5 sec^{-1} at 20°C) in the absence of K^+ (Glynn & Karlish, 1976).

In order to test whether labeling of the protein with 5-IAF has any influence on the kinetics of charge translocation, parallel experiments were carried out with unlabeled membrane fragments. Within the experimental error limits, no difference in the shape of the current transient could be detected between labeled and unlabeled membrane preparations. This finding is consistent with the observation that labeling of Na,K-ATPase with 5-IAF does not affect the enzymatic activity (Kapakos & Steinberg, 1982).

Comparison of Electrical and Optical Signals (Na^+ Media)

Previous studies with chymotrypsin-modified enzyme (Borlinghaus et al., 1987) led to the conclusion that the major charge-carrying step in the sodium limb of the transport cycle is the deocclusion reaction $(Na_3)E_1{-}P \rightarrow P{-}E_2 \cdot Na_3$, followed by release of Na^+ to the extracellular medium. In an analogous way, the optical experiments with chymotrypsin-treated protein described above indicate that the main fluorescence change after ATP-induced phosphorylation of the protein is associated with the same reaction sequence $(Na_3)E_1{-}P \rightarrow P{-}E_2 \cdot Na_3 \rightarrow P{-}E_2$.

The simplest situation for a comparison of optical and electrical signals is given when both the fluorescence change and the transient current result from a single reaction step $A \rightarrow B$. The fluorescence intensity F may then be represented by $F = f_A c_A + f_B c_B$, where f_A and f_B are the contributions of A and

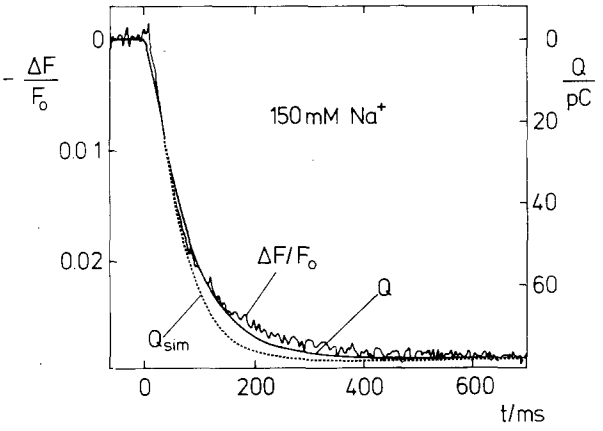

Fig. 12. Comparison of ATP-induced electrical and optical signals measured in parallel experiments under nearly identical conditions (150 mM Na^+, 30 mM imidazole, pH = 7.2, 1 mM EDTA, 10 mM Mg^{2+}, T = 21–22°C). $\Delta F/F_0$ is the relative fluorescence change and Q the translocated charge (Eq. (3)); 1 $pC \equiv 10^{-12}$ coulomb. Q_{sim} is the predicted value of the translocated charge, as obtained by numerical simulation of the reaction cycle of Fig. 15 with the parameter values of the Table, together with $c_P = c_D = c_K = 0$ and with the following assignments of the dielectric coefficients: $\alpha' = \alpha'' = \alpha_l = \alpha_r = 0$, $\alpha_p = 1$ (*see* text). In the fluorescent experiment the concentration of caged ATP was 100 μM and the concentration of released ATP was approximately 20 μM. In the current measurement the concentration of caged ATP was 240 μM and the concentration of released ATP about 30 μM

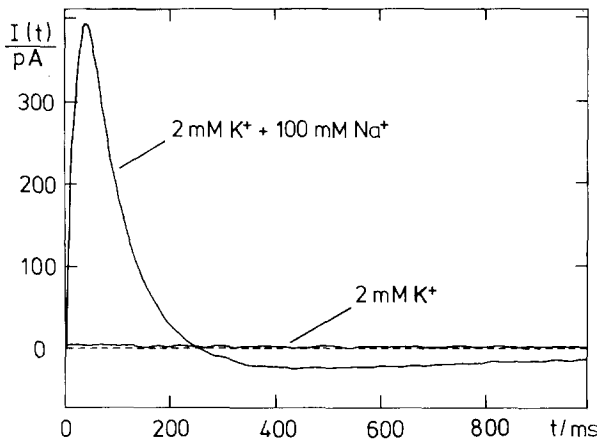

Fig. 13. Electrical transients in the presence of 2 mM K^+ alone and after addition of 100 mM Na^+. The transient was measured as a voltage signal and was subsequently transformed into a current $I(t)$ by digital differentiation. T = 25.5°C. The other experimental conditions were the same as in Fig. 11

B to F, and c_A and c_B are the concentrations. Introducing the initial fluorescence $F_0 = f_A c$, where $c = c_A + c_B$ is the total concentration, the time course of the relative fluorescence change $\Delta F/F_0 \equiv (F - F_0)/F_0$ is obtained as

$$\frac{\Delta F(t)}{F_0} = \frac{1}{c}\left(\frac{f_B}{f_A} - 1\right) c_B(t). \tag{1}$$

On the other hand, the transient pump current $I_p(t) - I_p^\infty$ associated with the reaction $A \rightarrow B$ may be written as

$$I_p(t) - I_p^\infty = a e_0 \frac{dc_B}{dt} \tag{2}$$

where e_0 is the elementary charge and a is a constant; I_p^∞ accounts for any quasistationary component of $I_p(t)$. According to Eq. (2), the total translocated charge $Q(t)$ is given by

$$Q(t) \equiv \int_0^t (I_p - I_p^\infty) = a e_0 c_B(t). \tag{3}$$

Comparison with Eq. (1) shows that under the assumptions introduced above, $\Delta F(t)/F_0$ and $Q(t)$ should exhibit the same time course, apart from a scaling factor.

A behavior predicted by Eqs. (1) and (3) is observed in experiments in K^+-free Na^+ media. This is shown in Fig. 12 in which $\Delta F(t)/F_0$ is plotted together with the translocated charge $Q(t)$ for c_N = 150 mM. $Q(t)$ was obtained according to Eq. (3) as the time integral of $I_p - I_p^\infty$. It is seen that $\Delta F(t)/F_0$ and $Q(t)$ nearly coincide. This indicates that both the fluorescence change as well as the charge translocation take place in the same reaction step. As discussed above, a likely candidate for this common reaction step is the deocclusion of sodium.

Electrical Signals in the Presence of K^+

When the medium contained 2 mM K^+, but no Na^+, the transient electric current following an ATP-concentration jump was virtually zero (Fig. 13). As seen from Fig. 13, subsequent addition of 100 mM Na^+ and photochemical ATP release gave rise to a large current signal. Similar results were obtained when the K^+ concentration was varied in the range between 1 and 10 mM. In some experiments, at high amplification, a small current signal could be detected in the presence of K^+ alone, exhibiting a biphasic shape with a peak at $t \approx$ 0–100 msec and a subsequent decline to zero. The signal was always positive (corresponding to translocation of positive charge towards the lipid bilayer), but the amplitude was subjected to considerable variations from experiment to experiment. It cannot be excluded that the spurious currents observed in K^+ media were caused by trace impurities of Na^+. As discussed

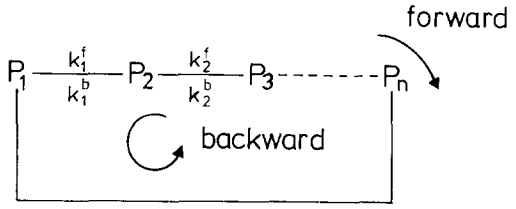

Fig. 14. Transitions between states $P_1, P_2, \ldots, P_n$ of a pump molecule. $k_1^f, k_2^f, \ldots$ and $k_1^b, k_2^b, \ldots$ are rate constants for transitions in foward and backward direction, respectively

previously (Läuger & Apell, 1986), intrinsic charge translocations other than movements of binding sites can contribute to the current signal. From the current transient under nominally Na^+-free conditions, the total translocated charge Q could be approximately determined. For this purpose the measured current $I(t)$ was transformed into the intrinsic pump current $I_p(t)$ as described above. The charge Q_∞ was obtained from the time integral of $I_p(t) - I_p^\infty$ between the limits $t = 0$ and $t \to \infty$. From a series of experiments of the kind represented in Fig. 13, the ratio ρ of translocated charge in the absence and in the presence of Na^+ was determined. The upper limit of $\rho \equiv Q_\infty(K)/Q_\infty(K + Na)$ was found to be approximately 0.01.

It is pertinent to note that the absence of a current transient under Na^+-free conditions is unlikely to be an artifact resulting from the inaccessibility of the extracellular side of the pump molecule facing the lipid bilayer. From previous studies (Glynn, 1985) it is known that in Na^+-free K^+ media, the Na,K-ATPase is present in the form $E_2(K_2)$ with occluded potassium (Fig. 1).

The transient currents represented in Figs. 11 and 13 are observed under single-turnover conditions in which the pump moves through part of the reaction cycle. From the Na^+ experiment (Fig. 11), it is clear that the sensitivity of the current measurement is sufficient to detect charge translocation under single-turnover conditions, and therefore a current signal should have been observed in the K^+ experiment (Fig. 13), if the transitions $E_2(K_2) \to K_2 \cdot E_1 \to E_1$ are associated with charge movement. In the optical experiment which was carried out under virtually identical conditions, a large fluorescence change was observed after the light flash (Fig. 9), indicating that an appreciable shift of the conformation equilibrium between $E_2(K_2)$ and $K_2 \cdot E_1$ occurs after ATP release. Comparison of the optical and electrical signals thus leads to the conclusion that the transition $ATP \cdot E_2(K_2) \to K_2 \cdot E_1 \cdot ATP$ is electrically silent.

Comparison of the Experimental Results with Theoretical Predictions

In the following we compare the experimental results with predictions derived from the Post-Albers reaction scheme. For this purpose, a numerical simulation of the transport cycle of Fig. 15 is carried out. The shape of the observed optical and electrical transients is found to agree with predictions from the reaction model, when the parameters of the model are chosen in an appropriate way.

Time Dependence of Fluorescence Signal $\Delta F/F_0$ and Pump Current I_p

The method for evaluating the time behavior of $\Delta F/F_0$ and I_p may be described on the basis of the general reaction scheme of Fig. 14 in which it is assumed that operation of the pump involves a sequence of transitions between states P_i ($i = 1, 2, \ldots n$). The rate constants k_i^f and k_i^b in forward and backward direction are, in general, pseudomonomolecular rate constants which may contain concentrations, such as ion or nucleotide concentrations. The kinetic behavior of the system may be described by introducing the fraction $x_i(t)$ of pump molecules in state P_i at time t. The time derivative of x_i is given by

$$dx_i/dt = -(k_{i-1}^b + k_i^f)x_i + k_{i-1}^f x_{i-1} + k_{i+1}^b x_{i+1}. \quad (4)$$

The n functions $x_i(t)$ are obtained by numerical integration of the n relations given by Eq. (4). If N is the number of pump molecules contributing to the fluorescence signal and φ_i is the fluorescence contribution of a single pump molecule in state P_i, the measured fluorescence intensity F (corrected for background radiation) may be represented by

$$F = N \sum_i \varphi_i x_i. \quad (5)$$

Introducing the initial values $x_{i0} \equiv x_i(0)$ of the quantities x_i (prior to the release of ATP) and the initial value F_0 of F, the relative change of fluorescence intensity, $\Delta F/F_0 \equiv (F - F_0)/F_0$, is obtained as

$$\frac{\Delta F}{F_0} = \frac{\sum_i f_i(x_i - x_{i0})}{1 + \sum_i f_i x_{i0}} \quad (6)$$

$$f_i \equiv (\varphi_i - \varphi_1)/\varphi_1. \quad (7)$$

The quantities f_i are the relative fluorescence increments of state i with respect to state 1.

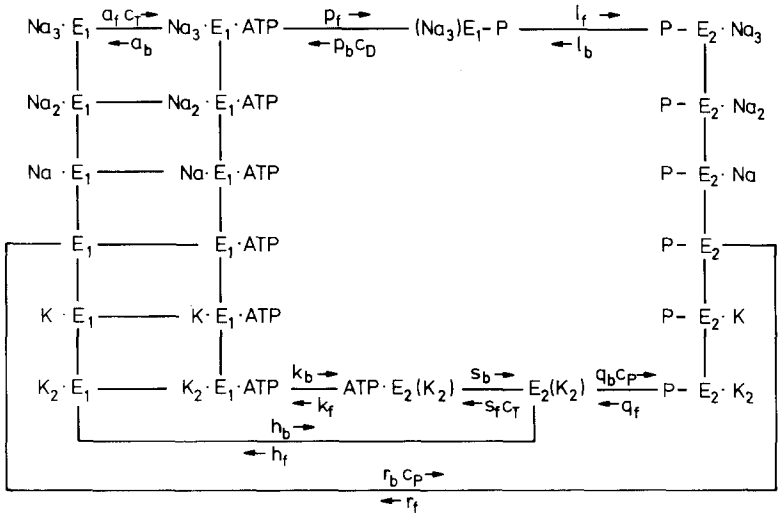

Fig. 15. Expanded form of the Post-Albers cycle (Fig. 1) for the evaluation of the time dependence of $\Delta F/F_0$ and of I_p. a_f, p_f, . . . and a_b, p_b, . . . are rate constants for transitions in forward and backward direction, respectively. c_T, c_D and c_P are the concentrations of ATP, ADP and P_i. The rate constants a_f and a_b are assumed to be the same for all transitions $Na_i \cdot E_1 \leftrightarrow Na_i \cdot E_1 \cdot ATP$ and $K_j \cdot E_1 \leftrightarrow K_j \cdot E_1 \cdot ATP$ ($i = 0, 1, 2, 3; j = 1, 2$)

In order to describe the time dependence of the transient pump current I_p, we introduce the net rate Φ_i of transitions $P_i \rightarrow P_{i+1}$ (referred to a single pump molecule):

$$\Phi_i = k_i^f x_i - k_{i+1}^b x_{i+1}. \tag{8}$$

The contribution of Φ_i to I_p may be written as $e_0 N \alpha_i \Phi_i$, where e_0 is the elementary charge and α_i the "dielectric coefficient" associated with transition $P_i \rightarrow P_{i+1}$ (Läuger et al., 1981). This yields

$$I_p = e_0 N \sum_i \alpha_i \Phi_i. \tag{9}$$

The essential microscopic information provided by $I_p(t)$ is contained in the dielectric coefficients α_i which depend on the magnitude of the translocated charge and on the distance over which the charge moves.

It should be noted that the validity of Eqs. (6) and (9) is not restricted to the simple reaction cycle of Fig. 14. It is easily seen that Eqs. (6) and (9) also apply to arbitrarily branched reaction schemes.

Reaction Model

The numerical analysis of Eqs. (6) and (9), which will be described below, is based on the Post-Albers cycle (Fig. 1) which is represented in more detailed form in Fig. 15. The reaction scheme of Fig. 15 is somewhat simplified insofar as additional phosphorylated states that have been postulated in the literature (Nørby, Klodos & Christiansen, 1983; Yoda & Yoda, 1986, 1987; Plesner & Plesner, 1988) are omitted. Furthermore, Fig. 15 does not explicitly account for transitions between the unliganded states E_1 and E_2. This seems justified, since the equilibrium between E_1 and E_2 lies far on the side of E_1 (Karlish & Stein, 1982). For the analysis of the reaction scheme we assume that ion-binding and -release steps are not rate-limiting and that Na^+ and ATP (as well as K^+ and ATP) bind independently to form E_1 of the protein (Karlish, Yates & Glynn, 1978*a*). This means that the following equilibrium relations hold at all times:

$$\frac{x[Na_i \cdot E_1]}{x[Na_{i-1} \cdot E_1]} = \frac{x[Na_i \cdot E_1 \cdot ATP]}{x[Na_{i-1} \cdot E_1 \cdot ATP]} = \frac{c_N}{K'_{Ni}} \equiv n_i' \tag{10}$$

$$\frac{x[K_j \cdot E_1]}{x[K_{j-1} \cdot E_1]} = \frac{x[K_j \cdot E_1 \cdot ATP]}{x[K_{j-1} \cdot E_1 \cdot ATP]} = \frac{c_K}{K'_{Kj}} \equiv k_j' \tag{11}$$

($i = 1, 2, 3; j = 1, 2$).

$x[A]$ denotes the fraction of pump molecules in state A. c_N and c_K are the concentrations of Na^+ and K^+, respectively, and K'_{Ni} and K'_{Kj} are equilibrium dissociation constants. Analogous equations hold for state $P{-}E_2$. The assumption of rapid binding and release of alkali ions has been introduced here to simplify the analysis. In view of recent experimental findings indicating that K^+ release from state $P{-}E_2 \cdot K_2$ may be slow (Forbush, 1987*b*), the equilibrium assumption should be replaced by a more realistic treatment as soon as more detailed kinetic information becomes available.

According to the principle of detailed balance, the rate constants and equilibrium constants are connected by the following relations, which correspond to three independent cycles in the reaction scheme of Fig. 15 (Läuger & Apell, 1986):

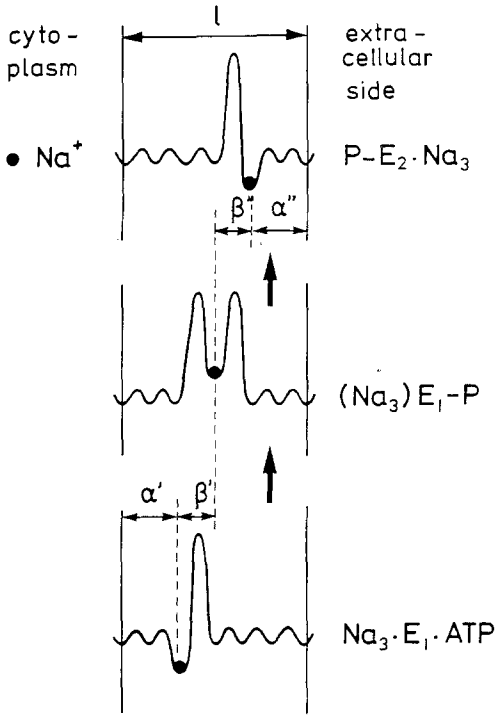

Fig. 16. Hypothetical energy profile of a sodium ion along the transport pathway. The ion binding sites in state $Na_3 \cdot E_1 \cdot ATP$ are connected with the cytoplasmic side by a series of low barriers, but separated from the extracellular medium by a high barrier. In the "occluded" state $(Na_3)E_1-P$ the energy barriers on either side are high. In state $P-E_2 \cdot Na_3$ the binding sites are easily accessible from the extracellular phase. α', α'', β', and β'' are dielectric distances, depending on the location of the ion binding site in the protein and on the dielectric properties of the protein and the surrounding medium

$$\frac{a_f k_b s_b h_f}{a_b k_f s_f h_b} = 1 \tag{12}$$

$$\frac{r_f q_b h_b}{r_b q_f h_f} \cdot \frac{K''_{K1} K''_{K2}}{K'_{K1} K'_{K2}} = 1 \tag{13}$$

$$\frac{p_f l_f r_f a_f}{p_b l_b r_b a_b} \cdot \frac{K''_{N1} K''_{N2} K''_{N3}}{K'_{N1} K'_{N2} K'_{N3}} = K. \tag{14}$$

$K \equiv \bar{c}_D \bar{c}_P / \bar{c}_T$ is the equilibrium constant of ATP hydrolysis ($\bar{c}_T$, $\bar{c}_D$ and $\bar{c}_P$ are equilibrium concentrations of ATP, ADP and P_i).

For the calculation of $\Delta F(t)/F_0$, the rate equations [Eq. (4)] are integrated under the initial condition [ATP] $\equiv c_T = 0$, as described in Appendix A. The time course of c_T after the light flash at $t = 0$ is assumed to be given by

$$c_T(t) = c_T^{\infty}[1 - \exp(-k_T t)]. \tag{15}$$

The quantity k_T represents an overall rate constant accounting for the release of ATP from caged ATP, as well as for the exchange of caged ATP for ATP at the nucleotide binding site of the protein (Forbush, 1984). For a more detailed analysis of the reactions preceding binding of ATP, *see* Apell et al. (1987).

Evaluation of $I_p(t)$

To calculate $I_p(t)$ from Eq. (9), the previously-described method for the evaluation of the net rates Φ_i may be used (Apell et al., 1987). The analysis is based on the following assumptions:

a) Binding and release of ATP is treated as electrically silent processes. This means that the dielectric coefficients of the processes $Na_i \cdot E_1 \rightarrow Na_i \cdot E_1 \cdot ATP, \ldots, K_j \cdot E_1 \rightarrow K_j \cdot E_1 \cdot ATP$ and $E_2(K_2) \rightarrow ATP \cdot E_2(K_2)$ are equal to zero.

b) The sodium binding sites and the potassium binding sites in state E_1 (and also in state E_2) are assumed to be electrically equivalent. Accordingly, the reactions $Na_{i-1} \cdot E_1 \rightarrow Na_i \cdot E_1$ ($i = 1, 2, 3$) and $K_{j-1} \cdot E_1 \rightarrow K_j \cdot E_1$ ($j = 1, 2$) are described by the same dielectric coefficient a', which accounts for the depth of the "ion well" (Mitchell & Moyle, 1974) at the cytoplasmic side (Fig. 16). In a similar way, ion binding at the extracellular side is described by a dielectric coefficient α''.

c) Intrinsic charge displacements in the protein (other than movements of the ion-binding sites) are neglected. This means that the dielectric coefficients corresponding to the reactions described by rate constants p, l, k and q in Fig. 15 given by

$$\alpha_p = (3 + z_L)\beta' \tag{16}$$

$$\alpha_l = (3 + z_L)\beta'' \tag{17}$$

$$\alpha_k = (2 + z_L)\gamma' \tag{18}$$

$$\alpha_q = (2 + z_L)\gamma''. \tag{19}$$

$z_L e_o$ is the charge of the empty ion-binding site, and β', β'', γ', γ'' are relative dielectric displacements as indicated in Fig. 16 (γ' and γ'' are defined in an analogous way as β' and β''). The quantities α', α'', ... are connected by the following relations (*compare* Fig. 16):

$$\alpha' + \alpha'' + \beta' + \beta'' = 1 \tag{20}$$

$$\alpha' + \alpha'' - \gamma' - \gamma'' = 1. \tag{21}$$

Since, according to assumption a), the coefficients α_a and α_s vanish, α_h and α_r are simply given by (*compare* Fig. 15):

$$\alpha_h = \alpha_k; \ \alpha_r = \alpha_q + \alpha_k. \tag{22}$$

Table. Values of kinetic parameters of the reaction scheme of Fig. 15, used for numerical simulation of $\Delta F(t)/F_o$ and $I_p(t)$; $T = 20°C$

Parameter	Value	Notes
K'_N	3 mM	*See* text
K''_N	200 mM	*See* text
K'_K	20 mM	*See* text
K''_K	1 mM	*See* text
K	4×10^5 M	a
p_f	180 sec^{-1}	b
p_b	2×10^4 M^{-1} sec^{-1}	c
l_f	19 sec^{-1}	d
l_b	1.7 sec^{-1}	d
q_f	500 sec^{-1}	e
q_b	5.8×10^6 M^{-1} sec^{-1}	e
s_f	2.5×10^6 M^{-1} sec^{-1}	f
s_b	140 sec^{-1}	f
k_f	15 sec^{-1}	g
k_b	670 sec^{-1}	h
a_f	10^7 M^{-1} sec^{-1}	i
a_b	20 sec^{-1}	Mårdh & Post (1977)
r_f	1 sec^{-1}	k
r_b	3.6×10^4 M^{-1} sec^{-1}	l
h_f	0.2 sec^{-1}	m
h_b	250 sec^{-1}	m

[a] Veech et al. (1979) give a value of $\Delta G_o = -32.4$ kJ/mol for the hydrolysis of ATP at pH 7.2, 1 mM Mg^{2+} and 38°C, corresponding to $K = 2.8 \times 10^5$ M. With $\Delta H = -25$ kJ/mol (Alberty, 1969), K becomes equal to 4.2×10^5 M at 20°C.

[b] Mårdh and Zetterquist (1974) obtained, at 21°C, a value of 180 sec^{-1} for the pseudo-first-order rate constant of phosphorylation of bovine brain microsomal Na,K-ATPase when neither Na^+ nor ATP were rate limiting.

[c] Estimated from Mårdh (1975); *compare* Läuger & Apell, 1986.

[d] l_f and l_b were estimated by fitting Eq. (6) to the observed time course of $\Delta F/F_o$. For bovine-brain enzyme, Mårdh (1975) obtained a value of $l_f \approx 80$ sec^{-1} at 21°C. The values of l_f and l_b of the Table approximately agree with the previous finding $l_f/l_b \approx 10$ (Mårdh, 1975; Glynn, 1984).

[e] q_f/q_b was calculated from Eq. (13) to be 0.086 mM, using the numerical values of r_f, r_b, . . . given in this Table. q_f was arbitrarily chosen to be 500 sec^{-1}, assuming that the reaction $P - E_2 \cdot K \rightarrow E_2(K_2)$ is not rate limiting; from deocclusion experiments, Forbush (1988) concluded that q_f is much larger than 100 sec^{-1} at pH 7.0. From $q_f/q_b = 0.086$ mM and $q_f = 500$ sec^{-1}, $q_b = 5.8 \times 10^6$ M^{-1} sec^{-1} is obtained.

[f] The value of s_f was arbitrarily chosen to be 2.5×10^6 M^{-1} sec^{-1}, assuming that ATP binding to $E_2(K_2)$ is not rate limiting at millimolar ATP concentrations. With $s_b = 140$ sec^{-1}, the ratio s_b/s_f becomes 56 μM. This is smaller than estimated values of 0.1–1 mM for the equilibrium dissociation constant of ATP at the low-affinity site (Robinson & Flashner, 1979; Moczydlowski & Fortes, 1981).

[g] From time-resolved fluorescence experiments, Karlish and Yates (1978) estimated for the transition $ATP \cdot E_2(K_2) \rightarrow K_2 \cdot E_2 \cdot ATP$ a rate of 50 sec^{-1} at 20°C. This value agrees with the rate of deocclusion of K^+ (45 sec^{-1} at 20°C) observed by Forbush (1987*a*) at saturating ATP concentration.

[h] Calculated from Eq. (12), using the numerical values of a_f, a_b, . . . given in this Table. Karlish and Yates (1978) observed a value of $k_b \approx 300$ sec^{-1} in the absence of Mg^{2+} and nucleotides.

[i] From $a_b \approx 20$ sec^{-1} and an effective value of the equilibrium dissociation constant of $a_b/a_f \approx 2$ μM, accounting for competion with caged ATP. The experimental value of a_b/a_f is of the order of 0.1 μM (Robinson & Flashner, 1979).

[k] Estimated by fitting Eq. (9) to the observed time course of I_p. Glynn and Karlish (1976) reported a value of $r_f \approx 5$ sec^{-1} at 20°C.

[l] Calculated from Eq. (11), using the values of p_f, p_b, . . . given in the Table.

[m] From optical determinations of rates of conformational transitions at 20°C, Karlish (1980) estimated h_f and h_b to be about 0.3 and 300 sec^{-1}, respectively. Glynn and Richards (1982) observed a rate constant h_f of spontaneous deocclusion of Rb^+ of about 0.2 sec^{-1} at 20°C; a similar value (0.1 sec^{-1}) was recently reported by Forbush (1987*b*).

Values of Kinetic Parameters

Some of the rate constants and equilibrium constants of the reaction scheme of Fig. 15 can be taken from the literature, as summarized in the Table. These assignments of numerical values have to be considered as tentative, however, since the kinetic parameters have been determined with Na,K-ATPase from different sources, such as brain or kidney medulla. In a few cases, literature values of kinetic parameters have been modified in order to improve the fit to the experimental results (Table). The values of q_f and s_f, for which no experimental estimates are available, have been adjusted.

Assuming that the ion-binding sites are identical and independent (Robinson, 1983), equilibrium dissociation constants of Na^+ and K^+ at the cytoplasmic side are given by

$$K'_{N1} = \frac{1}{3} K'_N;\ K'_{N2} = K'_N;\ K'_{N3} = 3K'_N \tag{23}$$

$$K'_{K1} = \frac{1}{2} K'_K;\ K'_{K2} = 2K'_K. \tag{24}$$

Analogous relations hold at the extracellular side. The factors 1/3, 3, 1/2 and 2 are the usual statistical factors describing binding equilibria in a system with multiple binding sites (Tanford, 1961). For a more detailed discussion of Na^+- and K^+-binding the Na,K-ATPase, *see* Karlish and Stein (1985) and Karlish, Rephaeli and Stein (1985). Numerical values of K'_N, K''_N, K'_K, K''_K have been estimated from the Na^+- and K^+-concentration dependence of the ATP-hydrolysis rate of Na,K-ATPase (Skou, 1975), as described previously (Läuger & Apell, 1986).

Numerical Simulations

Numerical simulations of the reaction model of Fig. 15 were carried out under the conditions of the dif-

ferent experiments described above. Since the concentrations of ADP and inorganic phosphate built up by hydrolysis of ATP are negligible within the time of the experiment, c_D and c_P were set equal to zero throughout. The same set of parameter values, as given in the Table, was found to reproduce, at least qualitatively, the shape of the observed fluorescence and current signals. We have not attempted an optimal fit to the experimental data, but rather have tried to carry out the analysis with a minimal number of assumptions. In particular, we have assumed that the different states of the cycle can be grouped into three classes with respect to the intrinsic fluorescence φ_i [Eq. (5)]:

φ_1: {all E_1 states, including $(Na_3)E_1-P$}
φ_2: {all $P-E_2$ states}
φ_3: {$E_2(K_2)$ and ATP · $E_2(K_2)$}.

The introduction of only three different fluorescence parameters φ_1, φ_2 and φ_3 corresponds to the notion that the fluorescence of the chromophore is mainly determined by the conformational state of the protein and is insensitive to the binding of ligands (Na^+, K^+, ATP). The assumption that the conformational state with occluded sodium has the same fluorescence as state E_1 is based on the finding that chymotrypsin modification of the protein, which blocks deocclusion of Na^+, abolishes the fluorescence change.

According to Eq. (6), the time course of $\Delta F/F_0$ is determined by the relative fluorescence increments $f_i \equiv (\varphi_i - \varphi_1)/\varphi_1$. Since f_i is referred to fluorescence state 1 (containing all E_1 states), the relation

$$f_1 \equiv 0 \tag{25}$$

holds. According to the assumption introduced above, f_2 and f_3 are given by:

$$f_2 = f(P-E_2 \cdot Na_i) = f(P-E_2 \cdot K_j) \tag{26}$$
$(i = 0, 1, 2, 3; j = 1, 2)$

$$f_3 = f(E_2(K_2)) = f(\text{ATP} \cdot E_2(K_2)). \tag{27}$$

Introducing into Eq. (6) the variables x_i defined in Appendix A, $\Delta F/F_0$ can be represented by

$$\frac{\Delta F}{F_0} = \frac{f_2(x_4 - x_{40}) + f_3(x_5 - x_{50} + x_6 - x_{60})}{1 + f_2 x_{40} + f_3(x_{50} + x_{60})}. \tag{28}$$

For fitting Eq. (28) to the experimental data, the following values of f_2 and f_3 have been used:

$$f_2 = -0.027; f_3 = -0.14. \tag{29}$$

f_2 has been evaluated from the experiments in the absence of K^+. Using the value of f_2, f_3 is obtained from the fluorescence signal in the presence of Na^+ and K^+.

With these values of f_2 and f_3 and with the parameters of the Table, the simulated fluorescence signals are found to reproduce approximately the time course of the signals recorded under the various experimental conditions. The results of the simulations are compared in Figs. 6, 8 and 10 with the experimental data. As seen from Fig. 6, the calculated dependence of signal amplitude a_F and half-time $t_{1/2}$ on Na^+ concentration c_N under K^+-free conditions agrees well with the experimental findings. At low c_N the rate of the $E_1 \rightarrow E_2$ transition is limited by the low concentration of $Na_3 \cdot E_1$, and $t_{1/2}$ is large. On the other hand, at saturating Na^+ concentrations, the time $t_{1/2}$ is determined by the rate of the deocclusion step $(Na_3)E_1-P \rightarrow P-E_2 \cdot Na_3$ (rate constant l_p); accordingly, $t_{1/2}$ approaches a constant value $(\ln 2)/l_f \approx 40$ msec at large c_N.

The low rate of the $E_1 \rightarrow E_2$ transition at small c_N also explains the sodium-concentration dependence of a_F (Fig. 6*A*), in the following way. For $c_N \rightarrow 0$, the rate of transitions $Na_3 \cdot E_1 \cdot \text{ATP} \rightarrow (Na_3)E_1-P \rightarrow P-E_2$ becomes comparable to the rate of spontaneous dephosphorylation ($P-E_2 \rightarrow E_1$, rate constant $r_f \approx 1\ \text{sec}^{-1}$). Under this condition, when the formation rate of $P-E_2$ is of the same order or smaller than the rate of decay back to conformation E_1, ATP release to the solution can only slightly shift the E_1/E_2 concentration ratio. This means that the signal amplitude a_F must vanish for $c_N \rightarrow 0$. On the other hand, at high c_N, where a large fraction of pump molecules accumulates in state E_2 after phosphorylation, a_F approaches the limiting value $f_2 = -0.027$ (Fig. 6*A*).

In the presence of both Na^+ and K^+, the amplitude $-a_F$ of the fluorescence signal is increased compared to the experiments with K^+-free media (Fig. 8). On the basis of the reaction scheme of Fig. 15, the increase of $-a_F$ is explained assuming that in the presence of K^+, the pump enters state $E_2(K_2)$ which has a lower fluorescence than $P-E_2$. The observed saturation of a_F with increasing K^+-concentration, which reflects high-affinity binding of K^+ to state $P-E_2$, agrees with the predictions from numerical simulations (Fig. 8*B*). The K^+-concentration dependence of the half-time $t_{1/2}$ is also reproduced by the simulated fluorescence signals (Fig. 8*A*).

An alternative explanation for the difference in signal amplitude with and without K^+ could consist in the assumption that f_2 and f_3 are nearly equal, but that in the absence of K^+ an appreciable fraction of the enzyme remains in state $(Na_3)E_1 - P$ after phosphorylation (Steinberg & Karlish, 1989). This possi-

bility seems unlikely, however, since in the absence of K^+ the signal amplitude was the same with 20 and 150 mM Na^+. Furthermore, assuming $f_2 \approx f_3$, we were unable to fit the observed dependence of $t_{1/2}$ on potassium concentration c_K (Fig. 8*B*).

In experiments with sodium-free potassium media, the half-time $t_{1/2}$ of the fluorescence signal is found to decrease with increasing K^+ concentration c_K, whereas the signal amplitude a_F reaches a maximum and decreases again at large c_K (Fig. 10). This behavior is also seen in the simulated fluorescence signals, as Fig. 10 shows. The origin of the maximum in $a_F = f(c_K)$ may be explained in the following way. After the concentration jump, ATP binds to state $E_2(K_2)$, inducing transitions ATP $\cdot$ $E_2(K_2) \rightarrow$ $K_2 \cdot E_1 \cdot$ ATP. At intermediate K^+ concentrations, the newly formed state $K_2 \cdot E_1 \cdot$ ATP is rapidly depopulated by dissociation of K^+, and virtually all initially present $E_2(K_2)$ is transformed into E_1, leading to a large fluorescence increase. At high K^+-concentration, however, a large proportion of the enzyme remains in state $K_2 \cdot E_1$ after the $E_2 \rightarrow E_1$ transition, from which it can return, with a rate constant $h_b \approx 250$ sec^{-1}, back to $E_2(K_2)$. This reduces the net amount of enzyme which undergoes the transition from $E_2(K_2)$ to E_1, and thus the amplitude a_F.

From the time-dependent pump current $I_p(t)$ the translocated charge $Q(t)$ can be evaluated. In Fig. 12 the experimental values of Q are compared with the charge Q_{sim} predicted by numerical simulation of the reaction cycle. The time course of Q_{sim} critically depends on the assumptions regarding the nature of the electrogenic steps. A satisfactory agreement between $Q(t)$ and $Q_{sim}(t)$ is found, assuming that formation of the occluded state ($Na_3 \cdot E_1 \cdot$ ATP $\rightarrow$ $(Na_3)E_1{-}P$) is an electrically silent process. This means that the main charge-translocating events are the deocclusion step and/or the release of Na^+ to the extracellular medium. The calculation of Q_{sim} was carried out with the parameter values of the Table, together with the following assignments of the dielectric coefficients. According to the finding that the reactions prior to the formation of the occluded state are electrically silent, α' and α_l (Eq. 17) were set equal to zero. Assuming that the major electrogenic event is the deocclusion step, α_p was set equal to unity and α'' equal to zero. (Since release of Na^+ is assumed to be fast, Q_{sim} is insensitive to the choice of α_p and α'', as long as the sum $\alpha_p + \alpha''$ remains constant.) From Eqs. (16), (17) and (20), it is seen that these assignments are equivalent to setting $\beta' = 1$, $\beta'' = 0$ and $z_L = -2$. The coefficients α_k and α_q (Eqs. (18) and (19)) are not to be specified, since the rate of the corresponding reactions vanishes in the absence of K^+. Furthermore, since the translocated charge is obtained from the difference $I_p - I_p^\infty$ (Eq. (3)), the coefficient α_f describing the back reaction responsible for the quasistationary pump-current I_p^∞ was set equal to zero. As seen from Fig. 12, the simulated and the observed time-course of translocated charge closely agree.

Discussion

Concentration-jump relaxation experiments yield information on the kinetic properties of an ion pump which cannot easily be obtained by other methods. In this study we have attempted to correlate transient electrical events in the Na,K-pump with conformational transitions elicited by an ATP-concentration jump. When the medium contains Na^+, but no K^+, the fluorescence of the 5-IAF-labeled protein decreases monotonously after activation by ATP. In parallel experiments carried out under otherwise identical conditions with membrane fragments bound to a planar bilayer, a transient pump current $I_p(t)$ was observed which decayed with nearly the same time behavior. Apart from a scaling factor, the fluorescence signal $\Delta F(t)/F_0$ was found to nearly superimpose with the time integral $Q(t)$ of I_p (Fig. 12). The close correlation between $\Delta F/F_0$ and $Q(t)$ indicates that the optical and the electrical transient are governed by the same rate-limiting step. Chymotrypsin modification of the protein, which is known to block the transition from (Na_3) $E_1{-}P$ to $P{-}E_2 \cdot Na_3$, was found to eliminate both the fluorescence signal and the current transient. This strongly suggests that the fluorescence change as well as the charge movement take place after formation of the occluded state, i.e., in the transitions $(Na_3)E_1{-}P \rightarrow P{-}E_2 \cdot Na_3 \rightarrow P{-}E_2$. Assuming that release of sodium ($P{-}E_2 \cdot Na_3 \rightarrow P{-}E_2$) is fast, the experimentally observed time constant of the fluorescence decay may be identified with the chemical relaxation time of the transition $(Na_3)E_1{-}P \rightleftarrows P{-}E_2 \cdot Na_3$.

In experiments with Na^+-free K^+-media, an inverse fluorescence change is observed after the ATP-concentration jump, which is likely to be associated with the transition $E_2(K_2) \rightarrow K_2 \cdot E_1$. In contrast to the large electrical signals observed in the presence of Na^+, no transient current could be detected when the medium contained only K^+. This finding indicates that the deocclusion step ($E_2(K_2)$ $\rightarrow K_2 \cdot E_1$) is electrically silent. The observation that Na^+ translocation is electrogenic, whereas K^+ translocation is electrically silent, can be explained assuming that the alkali-ion binding site of the protein bears a charge of $-2e_0$, corresponding to a net charge of $+e_0$ in the sodium-loaded form and a net charge of zero in the potassium-loaded form

(Goldshlegger et al., 1987; DeWeer, Gadsby & Roakowsky, 1988; Läuger & Apell, 1988).

After the transition $E_2(K_2) \rightarrow K_2 \cdot E_1$, K^+ ions are released to the cytoplasmic medium. Under the conditions of the experiment of Fig. 13 ($c_K = 2$ mM), net release occurs since the K^+ affinity in state E_1 is low ($K'_K \approx 20$ mM). The release step, $K_2 \cdot E_1 \rightarrow E_1$, could be associated with charge translocation, if the K^+ ions move in a narrow, low-conductance access channel ("ion well") connecting the binding site with the aqueous medium. The fact that no charge translocation is observed in the experiments with Na^+-free K^+ media provides strong arguments against the existence of a potassium well at the cytoplasmic side. It cannot be excluded, however, that a low-conductance access channel is present at the extracellular face of the pump.

It is well known (Glynn, 1985) that in the simultaneous presence of Na^+ and K^+, the phosphorylated state $P-E_2$ undergoes a rapid transformation into the occluded state $E_2(K_2)$ via the reaction sequence $P-E_2 \cdot Na_3 \rightarrow P-E_2 \cdot K_2 \rightarrow E_2(K_2)$. The fluorescence signal, which is observed in the presence of both Na^+ and K^+, exhibits the same time course as in the absence of K^+, but the amplitude of the decrease is much larger. These findings may be explained, assuming that $E_2(K_2)$ has a weaker fluorescence than $P-E_2 \cdot Na_3$ (Kapakos & Steinberg, 1986*a*) and that the transitions $P-E_2 \cdot Na_3 \rightarrow P-E_2 \cdot K_2 \rightarrow E_2(K_2)$ are fast compared with the preceding reaction step $(Na_3)E_1-P \rightarrow P-E_2 \cdot Na_3$.

The conclusions that we have drawn from our experiments may be compared with the results of previous studies. From voltage-jump current-relaxation experiments with cardiac cells, Nakao and Gadsby (1986) proposed that translocation of Na^+ is a major charge-carrying step in the pumping cycle of the Na,K-ATPase. Similar experiments gave evidence that translocation of K^+ is an electrically silent process (Bahinski, Nakao & Gadsby, 1988). Essentially the same conclusion has been drawn by Goldshlegger et al. (1987) from the finding that in reconstituted vesicles potassium-potassium exchange is voltage insensitive. These observations basically agree with the results of the present study.

The authors wants to thank Prof. W.D. Stein and Dr. R. Borlinghaus for valuable suggestions and M. Roudna for the preparation of Na,K-ATPase. This work has been financially supported by Deutsche Forschungsgemeinschaft (Sonderforschungsbereich 156).

References

Albers, R.W. 1967. Biochemical aspects of active transport. *Annu. Rev. Biochem.* **36**:727–756

Alberty, R.A. 1969. Standard Gibbs free energy, enthalpy, and entropy changes as a function of pH and pMg for several reactions involving adenosine phosphates. *J. Biol. Chem.* **244**:3290–3302

Apell, H.-J., Borlinghaus, R., Läuger, P. 1987. Fast charge translocations associated with partial reactions of the Na,K-pump: II. Microscopic analysis of transient currents. *J. Membrane Biol.* **97**:179–191

Bahinski, A., Nakao, M., Gadsby, D.C. 1988. Potassium translocation by the Na/K pump is voltage insensitive. *Proc. Natl. Acad. Sci. USA* **85**:3412–3416

Borlinghaus, R., Apell, H.-J. 1988. Current transients generated by the Na^+/K^+-ATPase after an ATP concentration jump: Dependence on sodium and ATP concentration. *Biochim. Biophys. Acta* **939**:197–206

Borlinghaus, R., Apell, H.-J., Läuger, P. 1987. Fast charge translocations associated with partial reactions of the Na,K-pump: I. Current and voltage transients after photochemical release of ATP. *J. Membrane Biol.* **97**:161–178

Cantley, L.C. 1981. Structure and mechanism of the (Na,K)-ATPase. *Curr. Top. Bioenerg.* **11**:201–237

Cantley, L.C., Carili, C.T., Smith, R.L., Perlman, D. 1984. Conformational changes of Na,K-ATPase necessary for transport. *Curr. Top. Membr. Transp.* **19**:315–322

De Luca, M., McElroy, W.D. 1978. Purification and properties of firefly luciferase. *Methods Enzymol.* **57**:3–15

De Weer, P., Gadsby, D.C., Rakowski, R.F. 1988. Voltage dependence of the Na-K pump. *Annu. Rev. Physiol.* **50**:225–241

Ernst, A., Böhme, H., Böger, P. 1983. Phosphorylation and nitrogenase activity in isolated heterocytes from *Anabaena variabilis*. *Biochim. Biophys. Acta* **723**:83–90

Fendler, K., Grell, E., Bamberg, E. 1987. Kinetics of pump currents generated by the Na^+/K^+-ATPase. *FEBS Lett.* **224**:83–88

Fendler, K., Grell, E., Haubs, M., Bamberg, E. 1985. Pump currents generated by the purified Na^+,K^+-ATPase from kidney on black lipid membranes. *EMBO J.* **4**:3079–3085

Forbush, B., III. 1984. Na^+ movement in a single turnover of the Na pump. *Proc. Natl. Acad. Sci. USA* **81**:5310–5314

Forbush, B., III. 1987*a*. Rapid release of ^{42}K and ^{86}Rb from an occluded state of the Na,K-pump in the presence of ATP or ADP. *J. Biol. Chem.* **262**:11104–11115

Forbush, B., III. 1987*b*. Rapid release of ^{42}K and ^{86}Rb from two distinct transport sites on the Na,K-pump in the presence of P_i or vanadate. *J. Biol. Chem.* **262**:11116–11127

Forbush, B., III. 1988. Rapid ^{86}Rb release from an occluded state of the Na,K-pump reflects the rate of dephosphorylation or dearsenylation. *J. Biol. Chem.* **263**:7961–7969

Fortes, P.A.G., Aguilar, R. 1988. Distance between 5-iodoacetamidofluorescein and the ATP and ouabain sites of (Na,K)-ATPase determined by fluorescence energy transfer. *In:* The Na^+,K^+-Pump. Part A: Molecular Aspects. J.C. Skou, J.G. Nørby, A.B. Maunsbach and M. Esman, editors. pp. 197–204. A.R. Liss, New York

Glynn, I.M. 1974. The electrogenic sodium pump. *In:* Electrogenic Transport. M.P. Blaustein and M. Lieberman, editors. pp. 33–48. Raven, New York

Glynn, I.M. 1985. The Na^+,K^+-transporting adenosine triphosphatase. *In:* The Enzymes of Biological Membranes. (2nd ed.) Vol. 3, pp. 35–114. A.N. Martonosi, editor. Plenum, New York

Glynn, I.M., Hara, Y., Richards, D.E. 1984. The occlusion of sodium ions within the mammalian sodium-potassium pump: Its role in sodium transport. *J. Physiol. (London)* **351**:531–547

Glynn, I.M., Hara, Y., Richards, D.E., Steinberg, M. 1987. Comparison of rates of cation release and of conformational change in dog kidney Na,K-ATPase. *J. Physiol. (London)* **383:**477–485

Glynn, I.M., Karlish, S.J.D. 1976. ATP hydrolysis associated with an uncoupled sodium flux through the sodium pump: Evidence for allosteric effects of intracellular ATP and extracellular sodium. *J. Physiol. (London)* **256:**465–496

Glynn, I.M., Richards, D.E. 1982. Occlusion of rubidium ions by the sodium-potassium pump: Its implications for the mechanism of potassium transport. *J. Physiol. (London)* **330:**17–43

Goldshlegger, R., Karlish, S.J.D., Rephaeli, A., Stein, W.D. 1987. The effect of membrane potential on the mammalian sodium-potassium pump reconstituted into phospholipid vesicles. *J. Physiol. (London)* **387:**331–355

Hegyvary, C., Jørgensen, P.L. 1981. Conformational changes of renal sodium plus potassium ion transport adenosine triphosphatase labeled with fluorescein. *J. Biol. Chem.* **256:**6296–6303

Jørgensen, P.L. 1974. Isolation of the (Na^+ + K^+)-ATPase. *Methods Enzymol.* **32:**277–290

Jørgensen, P.L. 1982. Mechanism of the Na^+,K^+ pump. Protein structure and conformations of the purified (Na^+ + K^+)-ATPase. *Biochim. Biophys. Acta* **694:**27–68

Jørgensen, P.L., Andersen, J.P. 1988. Structural basis for E_1 – E_2 conformational transitions in Na,K-pump and Ca-pump proteins. *J. Membrane Biol.* **103:**95–120

Jørgensen, P.L., Collins, J.H. 1986. Tryptic and chymotryptic cleavage sites in the sequence of α-subunit of (Na^+ + K^+)-ATPase from outer medulla of mammalian kidney. *Biochim. Biophys. Acta* **860:**570–576

Jørgensen, P.L., Karlish, S.J.D. 1980. Defective conformational response in a selectively trypsinized (Na^+ + K^+)-ATPase studied with tryptophan fluorescence. *Biochim. Biophys. Acta* **597:**305–317

Jørgensen, P.L., Petersen, J. 1985. Chymotryptic cleavage of α-subunit in E_1-forms of renal (Na^+ + K^+)-ATPase: Effects on enzymatic properties, ligand binding and cation exchange. *Biochim. Biophys. Acta* **821:**319–333

Kapakos, J.G., Steinberg, M. 1982. Fluorescent labeling of (Na^+ + K^+)-ATPase by 5-iodoacetamidofluorescein. *Biochim. Biophys. Acta* **693:**493–496

Kapakos, J.G., Steinberg, M. 1986*a*. Ligand binding to (Na,K)-ATPase labeled with 5-iodoacetamidofluorescein. *J. Biol. Chem.* **261:**2084–2089

Kapakos, J.G., Steinberg, M. 1986*b*. 5-Iodoacetamidofluorescein-labeled (Na,K)-ATPase. Steady-state fluorescence during turnover. *J. Biol. Chem.* **261:**2090–2096

Kaplan, J.H. 1985. Ion movements through the sodium pump. *Annu. Rev. Physiol.* **47:**535–544

Kaplan, J.H., Forbush, B., III, Hoffman, J.F. 1978. Rapid photolytic release of adenosine-5′-triphosphate from a protected analogue: Utilization by the Na : K pump of human red blood cell ghosts. *Biochemistry* **17:**1929–1935

Karlish, S.J.D. 1980. Characterization of conformational changes in (Na,K)ATPase labeled with fluorescein at the active site. *J. Bioenerg. Biomembr.* **12:**111–135

Karlish, S.J.D., Rephaeli, A., Stein, W.D. 1985. Transmembrane modulation of cation transport by the Na,K-pump. *In:* The Sodium Pump. I. Glynn and C.L. Ellory, editors. pp. 487–499. The Company of Biologists, Cambridge, U.K.

Karlish, S.J.D., Stein, W.D. 1982. Passive rubidium fluxes mediated by Na-K-ATPase reconstituted into phospholipid vesicles when ATP- and phosphate-free. *J. Physiol. (London)* **328:**295–316

Karlish, S.J.D., Stein, W.D. 1985. Cation activation of the pig kidney sodium pump: Transmembrane allosteric effects of sodium. *J. Physiol. (London)* **359:**119–149

Karlish, S.J.D., Yates, D.W. 1978. Tryptophane fluorescence of (Na^+ + K^+)-ATPase as a tool for study of the enzyme mechanism. *Biochim. Biophys. Acta* **527:**115–130

Karlish, S.J.D., Yates, D.W., Glynn, I.M. 1978*a*. Elementary steps of the (Na^+ + K^+)-ATPase mechanism, studied with formycin nucleotides. *Biochim. Biophys. Acta* **525:**230–251

Karlish, S.J.D., Yates, D.W., Glynn, I.M. 1978*b*. Conformational transitions between Na^+-bound and K^+-bound forms of (Na^+ + K^+)-ATPase, studied with formycin nucleotides. *Biochim. Biophys. Acta* **525:**252–264

Läuger, P., Apell, H.-J. 1986. A microscopic model for the current-voltage behaviour of the Na,K-pump. *Eur. Biophys. J.* **13:**305–321

Läuger, P., Apell, H.-J. 1988. Transient behaviour of the Na,K-pump: Microscopic analysis of nonstationary ion-translocation. *Biochim. Biophys. Acta* **944:**451–464

Läuger, P., Benz, R., Stark, G., Bamberg, E., Jordan, P.C., Fahr, A., Brock, W. 1981. Relaxation studies of ion transport systems in lipid bilayer membranes. *Q. Rev. Biophys.* **14:**513–598

Läuger, P., Lesslauer, W., Marti, E., Richter, J. 1967. Electrical properties of bimolecular phospholipid membranes. *Biochim. Biophys. Acta* **135:**20–32

Lindqvist, L. 1960. A flash photolysis study of fluorescein. *Ark. Kemi* **16:**79–138

Lowry, O.H., Rosebrough, N.J., Farr, A.L., Randall, R.J. 1951. Protein measurement with the Folin phenol reagents. *J. Biol. Chem.* **193:**265–275

Mårdh, S. 1975. Bovine brain Na^+,K^+-stimulated ATP phosphohydrolase studied by a rapid-mixing technique. K^+-stimulated liberation of [^{32}P] orthophosphate from [^{32}P] phosphoenzyme and resolution of the dephosphorylation into two phases. *Biochim. Biophys. Acta* **391:**448–463

Mårdh, S., Post, R.L. 1977. Phosphorylation from adenosine triphosphate of sodium- and potassium-activated adenosine triphosphatase. *J. Biol. Chem.* **252:**633–638

Mårdh, S., Zetterquist, Ö. 1974. Phosphorylation and dephosphorylation reactions of bovine brain (Na^+ + K^+)-stimulated ATP phosphohydrolase studied by a rapid-mixing technique. *Biochim. Biophys. Acta* **350:**473–483

McCray, J.A., Herbette, L., Kihara, T., Trentham, D.R. 1980. A new approach to time-resolved studies of ATP-requiring biological systems: Laserflash photolysis of caged ATP. *Proc. Natl. Acad. Sci. USA* **77:**7237–7241

Mitchell, P., Moyle, J. 1974. The mechanism of proton translocation in reversible proton-translocating adenosine triphosphatases, *Biochem. Soc. (Spec. Publ.)* **4:**91–111

Moczydlowski, E.G., Fortes, P.A.G. 1981. Inhibition of sodium and potassium adenosine triphosphatase by 2′,3′,-O-(2,4,6-trinitrocyclohexadienylidene) adenine nucleotide. *J. Biol. Chem.* **256:**2357–2366

Nagel, G., Fendler, K., Grell, E., Bamberg, E. 1987. Na^+ currents generated by the purified (Na^+ + K^+)-ATPase on planar lipid bilayers. *Biochim. Biophys. Acta* **901:**239–249

Nakao, M., Gadsby, D.C. 1986. Voltage dependence of Na translocation by the Na/K pump. *Nature (London)* **323:**628–630

Nørby, J.G., Klodos, I., Christiansen, N.O. 1983. Kinetics of Na-ATPase activity by the Na,K pump. *J. Gen. Physiol.* **82:**725–759

Plesner, L., Plesner, I.W. 1988. Distinction between the intermediates in Na^+-ATPase and Na^+,K^+-ATPase reactions: I. Ex-

change and hydrolysis kinetics at millimolar nucleotide concentrations. *Biochim. Biophys. Acta* **937**:51–62

Post, R.L., Hegyvary, C., Kume, S. 1972. Activation by adneosine triphosphate in the phosphorylation kinetics of sodium and potassium ion transport adenosine triphosphatase. *J. Biol. Chem.* **247**:6530–6540

Rephaeli, A., Richards, D., Karlish, S.J.D. 1986*a*. Conformational transitions in fluorescein-labeled (Na,K)ATPase reconstituted into phospholipid vesicles. *J. Biol. Chem.* **261**:6248–6254

Rephaeli, A., Richards, D., Karlish, S.J.D. 1986*b*. Electrical potential accelerates the $E_1P(Na)$-E_2P conformational transition of (Na,K)ATPase in reconstituted vesicles. *J. Biol. Chem.* **261**:12437–12440

Robinson, J.D. 1983. Kinetic analysis and reaction mechanism of the Na,K-ATPase. *Curr. Top. Membr. Transp.* **19**:485–512

Robinson, J.D., Flashner, M.S. 1979. The (Na^+ + K^+)-activated ATPase. Enzymatic and transport properties. *Biochim. Biophys. Acta* **549**:145–176

Schuurmans Stekhoven, F., Bonting, S.L. 1981. Transport adenosin-triphosphatases: Properties and function. *Physiol. Rev.* **61**:1–76

Schwartz, A., Nagano, K., Nakao, M., Lindenmayer, G.E., Allen, J.C. 1971. The sodium- and potassium-activated adenosinetriphosphatase system. *Methods Pharmacol.* **1**:361–388

Skou, J.C. 1975. The (Na^+ + K^+) activated enzyme system and its relationship to transport of sodium and potassium. *Q. Rev. Biophys.* **7**:401–431

Skou, J.C. 1982. The effect of pH, of ATP and of modification with pyridoxal-5-phosphate on the conformational transition between the Na^+-form and the K^+-form of the (Na^+ + K^+) ATPase. *Biochim. Biophys. Acta* **688**:369–380

Skou, J.C., Esmann, M. 1981. Eosin, a fluorescent probe of ATP binding to the (Na^+ + K^+)-ATPase. *Biochim. Biophys. Acta* **647**:232–240

Skou, J.C., Esmann, M. 1983. Effect of magnesium ions on the high-affinity binding of eosin to the (Na^+ + K^+)-ATPase. *Biochim. Biophys. Acta* **727**:101–107

Steinberg, M., Karlish, S.J.D. 1989. Studies on conformational changes in Na,K-ATPase labeled with 5-iodoacetamidofluorescein. *J. Biol. Chem.* **264**:2726–2734

Suzuki, K., Taniguchi, K., Iida, S. 1987. The acceleration of Na^+,K^+-ATPase activity by ATP and ATP analogues. *J. Biol. Chem.* **262**:11752–11757

Tanford, C. 1961. Physical Chemistry of Macromolecules. Chap. 8. John Wiley & Sons, New York

Taniguchi, K., Suzuki, K., Iida, S. 1983. Stopped flow measurement of conformational change induced by phosphorylation in (Na^+,K^+)-ATPase modified with N[*p*-(2-benzimidazolyl)phenyl]maleimide. *J. Biol. Chem.* **258**:6927–6931

Tyson, P.A., Steinberg, M., Wallick, E.T., Kirley, T.L. 1989. Identification of the 5-iodoacetamidofluorescein reporter site on the Na,K-ATPase. *J. Biol. Chem.* **264**:726–734

Veech, R.L., Lawson, J.W.R., Cornell, N.W., Krebs, H.A. 1979. Cytosolic phosphorylation potential. *J. Biol. Chem.* **254**:6538–6547

Yoda, S., Yoda, A. 1986. ADP- and K^+-sensitive phosphorylated intermediate of Na,K-ATPase. *J. Biol. Chem.* **261**:1147–1152

Yoda, A., Yoda, S. 1987. Two different phosphorylation-dephosphorylation cycles of Na,K-ATPase proteoliposomes accompanying Na^+ transport in the absence of K^+. *J. Biol. Chem.* **262**:110–115

Received 11 January 1989

Appendix A

Numerical Simulation of the Reaction Cycle of Fig. 15

We denote the fraction of pump molecules in state A by $x[A]$ and introduce the following variables:

$$x_1 \equiv x[Na_3 \cdot E_1] + x[Na_2 \cdot E_1] + x[Na \cdot E_1] + x[E_1] + x[K \cdot E_1] + x[K_2 \cdot E_1] \quad (A1)$$

$$x_2 \equiv x[Na_3 \cdot E_1 \cdot ATP] + x[Na_2 \cdot E_1 \cdot ATP] + x[Na \cdot E_1 \cdot ATP] + x[E_1 \cdot ATP] + x[K \cdot E_1 \cdot ATP] + x[K_2 \cdot E_1 \cdot ATP] \quad (A2)$$

$$x_3 \equiv \chi[(Na_3)E_1{-}P] \quad (A3)$$

$$x_4 \equiv x[P{-}E_2 \cdot Na_3] + x[P{-}E_2 \cdot Na_2] + x[P{-}E_2 \cdot Na] + x[P{-}E_2] + x[P{-}E_2 \cdot K] + x[P{-}E_2 \cdot K_2] \quad (A4)$$

$$x_5 \equiv x[E_2(K_2)] \quad (A5)$$

$$x_6 \equiv x[ATP \cdot E_2 \cdot (K_2)] \quad (A6)$$

$$x_1 + x_2 + x_3 + x_4 + x_5 + x_6 = 1. \quad (A7)$$

According to Fig. 15, the rate of change of x_1 is given by

$$\dot{x}_1 = -(a_f c_T + h_b k_1' k_2'/P' + r_b c_P/P')x_1 + a_b x_2 + (r_f/P'')x_4 + h_f x_5. \quad (A8)$$

Analogous equations hold for $\dot{x}_2, \dot{x}_3, \ldots, \dot{x}_6$.

In Eq. (A8) the following relations have been used which are obtained from Eqs. (10) and (11):

$$x[E_1] = \frac{x_1}{P'};\ x[K_2 \cdot E_1] = \frac{k_1' k_2'}{P'} x_1$$

$$x[P{-}E_2] = \frac{x_4}{P''} \quad (A9)$$

$$P' \equiv 1 + n_1' + n_1' n_2' + n_1' n_2' n_3' + k_1' + k_1' k_2' \quad (A10)$$

$$P'' \equiv 1 + n_1'' + n_1'' n_2'' + n_1'' n_2'' n_3'' + k_1'' + k_1'' k_2''. \quad (A11)$$

The differential equations for $\dot{x}_1, \ldots, \dot{x}_6$ may be numerically integrated using a Runge-Kutta algorithm. In this way the time course of the fluorescence signal $\Delta F/F_0$ may be evaluated using Eq. (3).